Int J Earth Sci (Geol Rundsch) (2014) 103:1359–1383
DOI 10.1007/s00531-013-0961-x

ORIGINAL PAPER

Armorican provenance for the mélange deposits below the Lizard ophiolite (Cornwall, UK): evidence for Devonian obduction of Cadomian and Lower Palaeozoic crust onto the southern margin of Avalonia

Rob A. Strachan · Ulf Linnemann · Teresa Jeffries · Kerstin Drost · Jens Ulrich

Received: 31 January 2013 / Accepted: 8 September 2013 / Published online: 28 September 2013

Abstract Devonian sedimentary rocks of the Meneage Formation within the footwall of the Lizard ophiolite complex in SW England are thought to have been derived from erosion of the over-riding Armorican microplate during collision with Avalonia and the closure of the Rheic Ocean. We further test this hypothesis by comparison of their detrital zircon suites with those of autochthonous Armorican strata. Five samples analysed from SW England (Avalonia) and NW France (Armorica) have a bimodal U–Pb zircon age distribution dominated by late Neoproterozoic to middle Cambrian (c. 710–518 Ma) and Palaeoproterozoic (c. 1,800–2,200 Ma) groupings. Both can be linked with lithologies exposed within the Cadomian belt as well as the West African craton, which is characterized by major tectonothermal events at 2.0–2.4 Ga. The detrital zircon signature of Avalonia is distinct from that of Armorica in that there is a much larger proportion of Mesoproterozoic detritus. The common provenance of the samples is therefore consistent with: (a) derivation of the Meneage Formation mélange deposits from the Armorican plate during Rheic Ocean closure and obduction of the Lizard Complex and (b) previous correlation of quartzite blocks within the Meneage Formation with the Ordovician Grès Armoricain Formation of NW France.

Keywords Armorica · Avalonia · Meneage Formation · Lizard ophiolite · Detrital zircons · Rheic Ocean

R. A. Strachan (✉)
School of Earth and Environmental Sciences, University of Portsmouth, Portsmouth PO1 3QL, UK
e-mail: rob.strachan@port.ac.uk

U. Linnemann · J. Ulrich
Senckenberg Naturhistorische Sammlungen Dresden, Museum für Mineralogie und Geologie, Königsbrücker Landstraße 159, 01109 Dresden, Germany

T. Jeffries
The Natural History Museum, Cromwell Road, London SW7 5BD, UK

K. Drost
Fachbereich Geowissenschaften, Isotopengeochemie, Universität Tübingen, Wilhelmstraße 56, 72076 Tübingen, Germany

Introduction

Armorica is one of a number of terranes (collectively termed peri-Gondwanan) that were located along the northern Gondwanan margin during the late Neoproterozoic (Fig. 1). Together, these terranes record a protracted (c. 780–600 Ma) history of subduction followed at c. 600–550 Ma by a diachronous transition to a continental San Andreas-type transform fault environment, which terminated orogenic activity. In Armorica, this period of orogenic activity is referred to as the Cadomian Orogeny (Bertrand 1921). Development of a stable platform environment followed in the Early Cambrian (e.g. Murphy and Nance 1989, 1991; Taylor and Strachan 1990; Nance et al. 1991, 2002, 2007; Murphy et al. 2000; Keppie et al. 2003). One of these terranes, Avalonia, rifted from the Gondwanan margin during the early Ordovician (Cocks and Torsvik 2002). The subsequent northward drift of Avalonia was associated with the closure of the Iapetus Ocean and the eventual collision of Avalonia with Baltica and Laurentia during the late Ordovician to Silurian to result in the Caledonian orogeny (Pickering et al. 1988; Soper et al. 1992). As Avalonia moved northwards, its southern trailing margin faced a progressively widening oceanic tract known as

Fig. 1 Geological map of the Central European Variscides (modified from Ballevre et al. 2009)

the Rheic Ocean (e.g. van Staal et al. 1998; Cocks and Torsvik 2002; Stampfli and Borel 2002). The later northward movement of Gondwana and its marginal terranes resulted in closure of the Rheic Ocean during the Devonian-Carboniferous to result in the Variscan orogeny (e.g. Matte 1986). The Rheic Ocean in NW Europe probably closed by south-directed subduction and the collision of Armorica with the southern margin of Avalonia resulted in a north-vergent fold and thrust belt in SW England and southern Ireland (Fig. 1; Holder and Leveridge 1986). The Rheic suture is thought to be represented in southwest England (Avalonia) by the ophiolitic rocks of the Lizard Complex (Fig. 1) (Nance et al. 2010 and references therein).

Dating of detrital zircons is a powerful tool that can be used to establish the likely provenance of clastic sedimentary rocks and hence assists in the development of palaeogeographic reconstructions (e.g. Rainbird et al. 2001; Fernández-Suárez et al. 2002a, b; Cawood et al. 2003, 2004, 2007; Murphy et al. 2004; Samson et al. 2005). This is particularly useful where terranes have been detached from their source regions by transcurrent faulting and/or continental rifting and ocean formation. Along the northern Gondwanan margin, for example, the contrasting tectonothermal histories of the Amazonian and West African cratons provide a test for deducing the original location of terranes along that margin (e.g. Fernández-Suárez et al. 2002a, b; Samson et al. 2005). In this paper, we

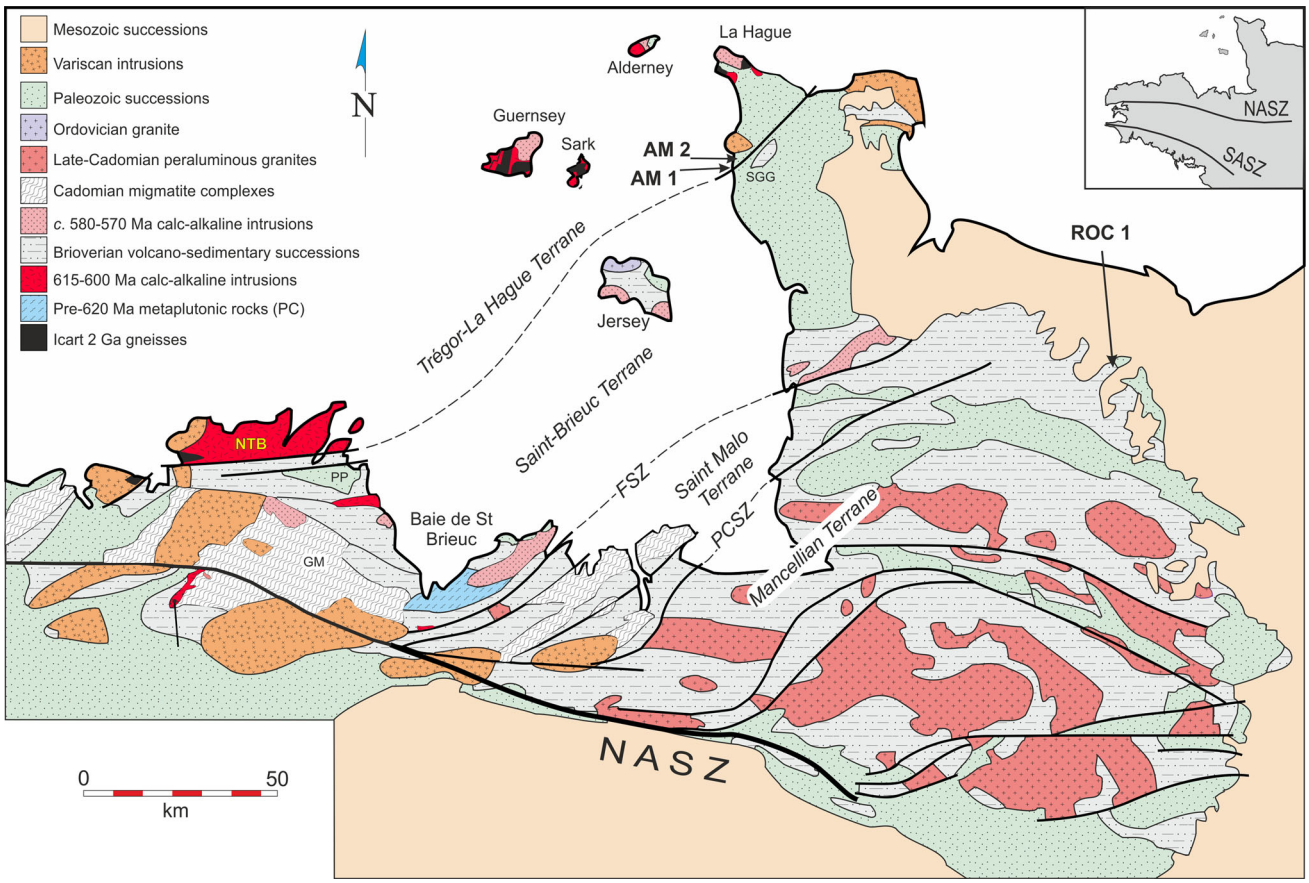

Fig. 2 Generalized geological map of the North Armorican Massif (modified from Linnemann et al. 2008) and sample locations (ROC 1, AM 1, AM 2). *FSZ* Fresnaye shear zone, *PCSZ* Plouer-cancale shear zone. *Inset* shows the North Armorican shear zone (NASZ) and South Armorican shear zone (SASZ). *C* Coutances, *GM* Guingamp migmatites, *NTB* North Trégor Batholith, *PC* Penthièvre Complex, *PP* Plourivo-Plouézec, *SGG* Saint Germain le-Gaillaird

present detrital zircon data from Cambrian and Ordovician clastic sedimentary rocks in Armorica (Normandy, NW France) and compare these data with those for rock units of a similar age in other peri-Gondwanan terranes. We also present detrital zircon data from clastic sedimentary rocks within the footwall of the Lizard Complex in SW England. These rock units are thought to have been derived from erosion of the over-riding Armorican microplate during the closure of the Rheic Ocean (Holder and Leveridge 1986; Dörr et al. 1999), and we further test this hypothesis by the comparison of their detrital zircon suites with those characteristic of autochthonous Armorican strata.

General geology

NW France (Armorica)

NW France and the Channel Islands together form the type area of the late Neoproterozoic Cadomian orogenic belt (e.g. Chantraine et al. 1994; Egal et al. 1996; Strachan et al. 1996; Linnemann et al. 2008). This belt is dominated by calc-alkaline plutons and volcanics and variably deformed and metamorphosed volcano-sedimentary sequences of the Brioverian Supergroup (Fig. 2). Small areas of Palaeoproterozoic Icartian basement have yielded U–Pb zircon ages of c. 2.2–1.8 Ga for the igneous protoliths (Calvez and Vidal 1978; Samson and D'Lemos 1998). These basement rocks have been correlated with the c. 2.0 Ga Eburnian belt of NW Africa and may represent a detached fragment of the Gondwanan margin (e.g. Cogné 1990; Rabu et al. 1990). Evolution of the Cadomian belt can be divided into four broad phases: (a) early subduction-related magmatism (750 and 670–660 Ma); (b) syn-kinematic calc-alkaline plutonism (615–600 Ma); rifting and accumulation of the Brioverian Supergroup (590–570 Ma) and (c) regional deformation and metamorphism and continued magmatism (570–540 Ma) (Linnemann et al. 2008 and references therein).

The Cadomian belt is overlain unconformably by transgressive sequences of Cambrian sandstones, siltstones and limestones. These rocks were deposited in fluvial-deltaic to shallow marine environments in basins that were

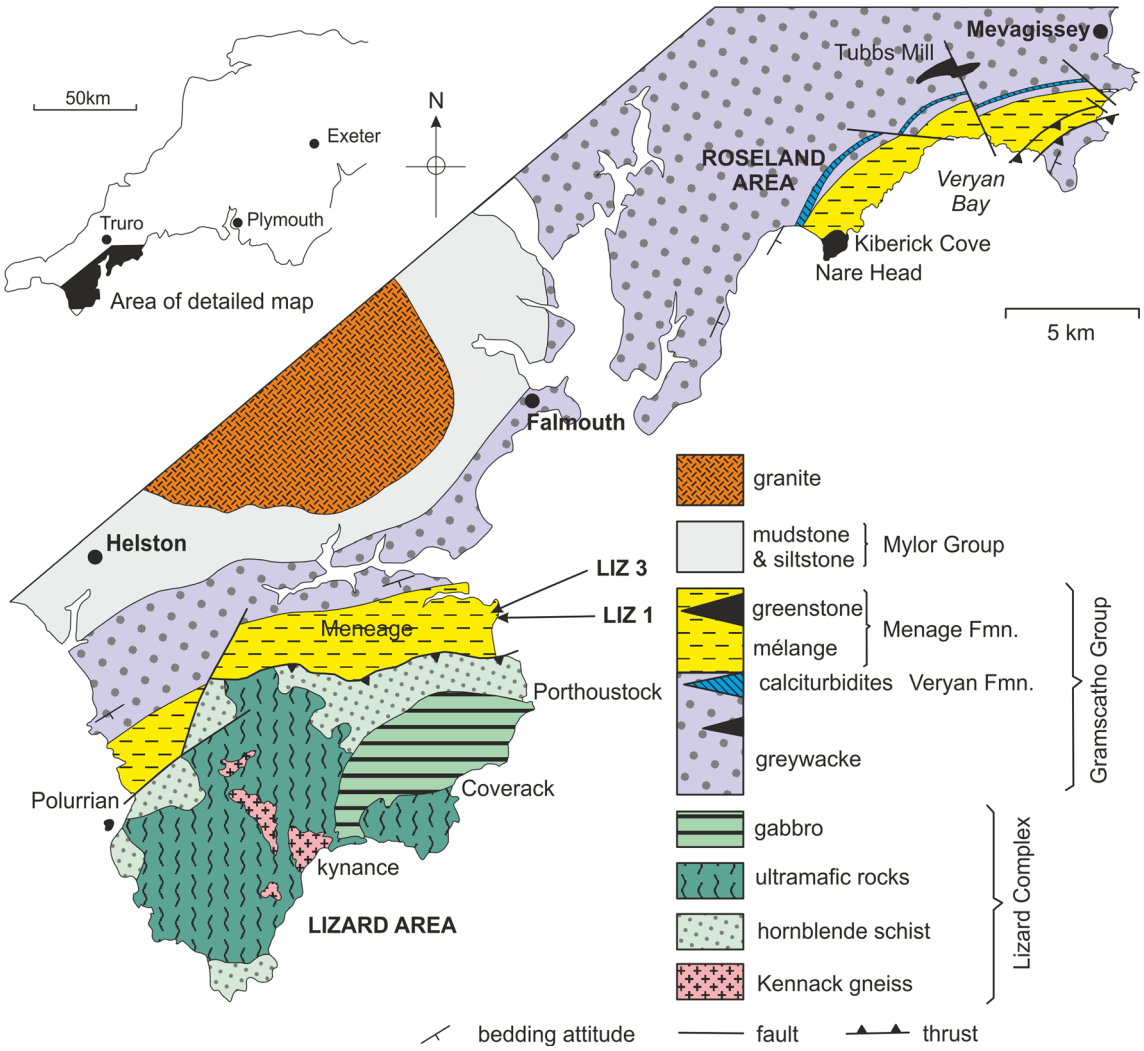

Fig. 3 Generalized map of the Lizard area and sample locations (LIZ 1, LIZ 3) (modified from Barnes and Andrews 1986)

separated from each other by broad landmasses that represented the residual topography after the final stages of Cadomian thickening (Doré 1994). Local occurrences of felsic volcanics are thought to represent the final stages of subduction-related magmatism (Chantraine et al. 1994). During the Arenig, a major marine transgression flooded most of Armorica and deposited an areally extensive quartz sandstone known as the Grès Armoricain Formation (Robardet et al. 1994). This formation is known informally as the 'Armorican Quartzite' and correlative units were also deposited in areas thought to have been contiguous with Armorica such as Iberia, Bohemia, Corsica, Turkey and parts of NW Africa.

One sample of a graywacke turbidite from the Brioverian Supergroup, Sample ROC 1, was collected in Normandy in NW France (Fig. 2). Two samples of the Lower Palaeozoic succession in NW France were also collected in Normandy (Fig. 2). Sample AM 1 is a quartzite from Lower Cambrian Le Rozel Formation. Sample AM 2 is a quartz sandstone collected from the Grès Armoricain Formation.

SW England (Avalonia)

The geology of SW England (Fig. 3) is dominated by Devonian and Carboniferous sedimentary successions with minor volcanic units. These rocks were deformed and metamorphosed at low to medium grades during the development of the Variscan fold and thrust belt (e.g. Shackleton et al. 1982; Coward and McClay 1983; Leveridge et al. 1984; Sanderson 1984; Seago and Chapman 1988). Deformation commenced at the end of the Devonian or during the early Carboniferous and migrated northwards. As the wave of deformation spreads northwards, the thickening orogenic wedge loaded the lithosphere and flexed down the foreland. The Devonian rift basin successions that were deposited on the southern passive

margin of Avalonia were succeeded by Carboniferous clastic sediments that accumulated in foreland basins which were also progressively deformed (Hartley 1993). The post-tectonic S-type granites of the Cornubian Batholith were emplaced during the late Carboniferous to early Permian (Chen et al. 1993; Chesley et al. 1993).

The structurally highest levels of the Variscan belt in SW England are represented by undated orthogneisses of the Eddystone reefs which are assumed to be part of the overriding Armorican plate (Holder and Leveridge 1986). The underlying Lizard Complex has long been recognized as a tectonically dismembered ophiolite (e.g. Bromley 1979; Styles and Kirby 1980; Vearncombe 1980; Barnes and Andrews 1984, 1986; Floyd 1984; Gibbons and Thompson 1991; Roberts et al. 1993). Its age is best constrained by a U–Pb zircon age of 397 ± 2 Ma obtained from a plagiogranite (Clark et al. 1998). A southerly inclined crustal-scale structure is interpreted as a Variscan (Rheic) suture which at surface corresponds to the Lizard Complex thrust system (BIRPS and ECORS 1986; Le Gall 1990).

The Devonian rocks that lie in the footwall of the Lizard Complex preserve a record of the closure of the Rheic Ocean (Nance et al. 2010). A major period of extensional rifting was initiated during the middle Devonian (Bluck et al. 1988, 1992). East–west-trending normal faults downthrowing to the south separated marine shelf and fluvial basins in the north of Cornwall from the deep-water Gramscatho Basin to the south. The latter is dominated by the turbiditic sandstones and mudstones of the Gramscatho Group. The basin was filled from the south by turbidites derived from the erosion of advancing nappes (Floyd and Leveridge 1987). The turbidite successions include sedimentary mélanges of the Meneage Formation (Barnes 1983), which also contain blocks of MORB-type volcanics and mica schist as well as large (200 m) quartzite blocks with Ordovician faunas that are closely comparable with the Grès Armoricain of northwest France (Sadler 1974). Two granite pebbles within the Meneage Formation yielded U–Pb zircon lower intercept ages of 373 ± 6 and 422 ± 4 Ma, which were interpreted as protolith ages (Dörr et al. 1999). The upper intercept ages of 2,606 ± 40 and 2,445 ± 19 Ma were thought to indicate the presence of an inherited Neoarchaean or Palaeoproterozoic source terrane. Together the data suggest derivation from a magmatic arc that developed on the leading edge of the Armorican plate (Dörr et al. 1999).

Two samples were analysed for the present study, both collected from the Meneage Formation north of Porthallow (Figs. 3, 4a). Sample LIZ 1 is a Devonian sandstone that forms the matrix of a debris-flow deposit (Fig. 4c). Sample

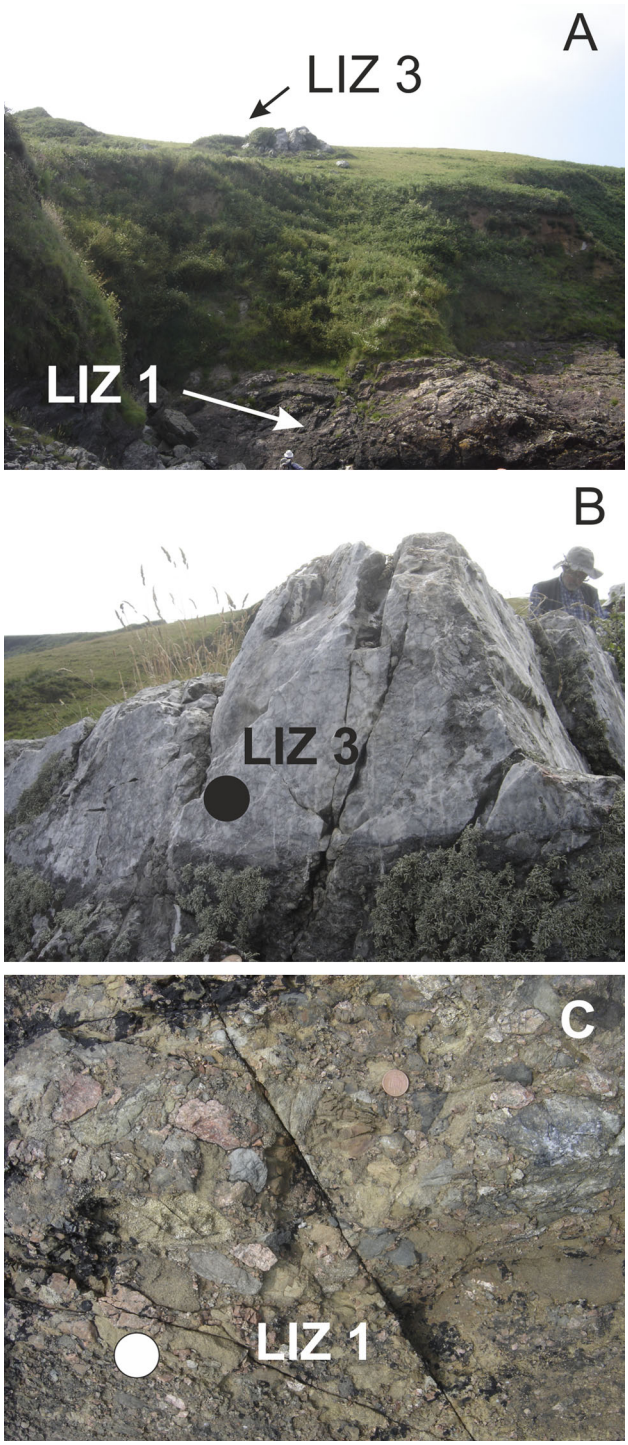

Fig. 4 Photographs from the sampling site in the Lizard area (samples LIZ 1 and LIZ 3, Meneage Formation, Gramscatho Group, Devonian, see also Fig. 3). **a** Meneage Formation and olistolith of a Lower Ordovician quartzite (Nare Cove, c. 1.3 km N of Porthallow), **b** Olistolith of the Lower Ordovician quartzite, sample LIZ 3), **c** Mélange deposit of the Meneage Formation, sample LIZ 1 was taken from the sandstone matrix)

LIZ 3 is an exotic quartzite block (Fig. 4b), part of the suite correlated by previous workers with the Ordovician Grès Armorican in Normandy.

Analytical techniques

Zircon preparation

Zircon concentrates were separated at the Museum für Mineralogie und Geologie (Senckenberg Naturhistorische Sammlungen Dresden). Fresh 1 kg samples of sandstone were crushed and sieved and then a heavy mineral separate was concentrated by the use of a heavy liquid (lithium heteropolytungstates in water). A final concentration was made by magnetic separation in a Frantz isodynamic separator. Selection of the zircon grains for U–Pb dating was achieved by hand picking under a binocular microscope. All zircon grains are either rounded or sub-rounded. Zircon grains of all sizes and morphological types were selected for single grain analysis by LA-ICP-MS. Zircon crystals were set in synthetic resin mounts, polished to approximately half their thickness and cleaned in a warm dilute HNO_3 ultrasonic bath followed by rinsing in de-ionized water. Cathodoluminescence images of selected zircon grains are presented in Fig. 5.

LA-ICP-MS U–Pb dating: U–Pb age determination of single grains was determined by LA-ICP-MS at the Natural History Museum, London, using a New-Wave UP213 frequency quintupled solid-state Nd:YAG laser ($\lambda = 213$ nm) coupled to a PlasmaQuad 3 quadrupole ICP-MS. Samples and standard were placed in an airtight chamber which was flushed by helium gas carrying the ablated material to the ICP-MS, mixed with Ar prior to injection to the plasma torch. U–Pb and Pb–Pb ratios of the unknowns were determined relative to that of the 91500 zircon standard with certified ID-TIMS ages of 1,062.4 ± 0.4 Ma for $^{206}Pb/^{238}U$ and 1,065.4 ± 0.3 Ma for $^{207}Pb/^{206}Pb$ (Wiedenbeck et al. 1995). Collection of data spanned up to 180 s per analysis and includes a gas background taken during the initial c. 60 s. To reduce the extent of inter-element laser-induced fractionation, the sample was moved relative to the laser beam along a line. The nominal diameter of the laser beam was 60 μm for the standard and 30 or 45 μm for the unknowns. Pulse energy of the laser was 0.03–0.06 mJ per pulse for the unknowns and 0.09 mJ per pulse for the standards with an energy density of 3.5 J/cm^2 and a repetition rate of 20 Hz. Only well-preserved zones within individual grains were analysed (Fig. 5), in order to escape metamorphic rims and altered domains. Further discussion of the analytical protocols used in this study can be found in Fernández-Suárez et al. (2002a) and Jeffries et al. (2003).

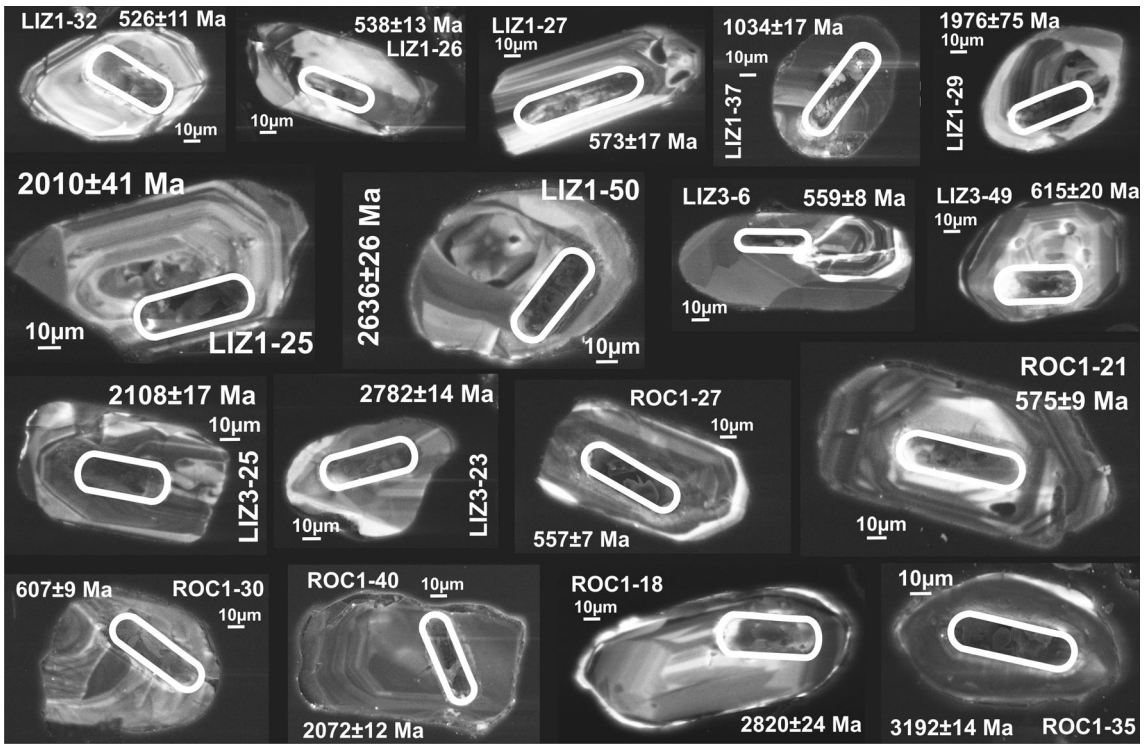

Fig. 5 Cathodoluminescence images of selected zircon grains from samples ROC 1, LIZ 1 and LIZ 3. For grains younger than 1 Ga, the $^{206}Pb/^{238}Pb$ age is quoted. For grains older than 1 Ga, the $^{207}Pb/^{206}Pb$ age is used

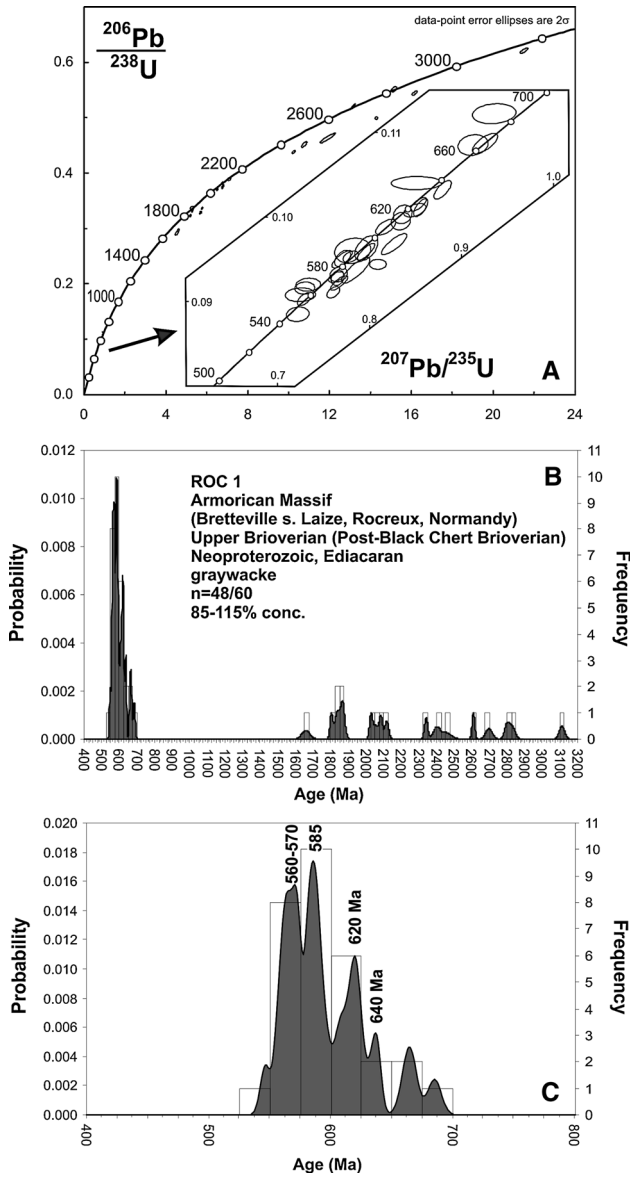

Fig. 6 U–Pb ages of detrital zircon grains from sample ROC 1 (graywacke, Upper Brioverian, Post-Bedded Chert Brioverian, Ediacaran, Rocreux near Bretteville s. Laize, Normandy, Armorican Massif). Concordia diagram (**a**) and combined binned frequency and probability density distribution plots of detrital zircon grains in the range of 400–3,200 Ma (**b**) and of 400–800 Ma (**c**)

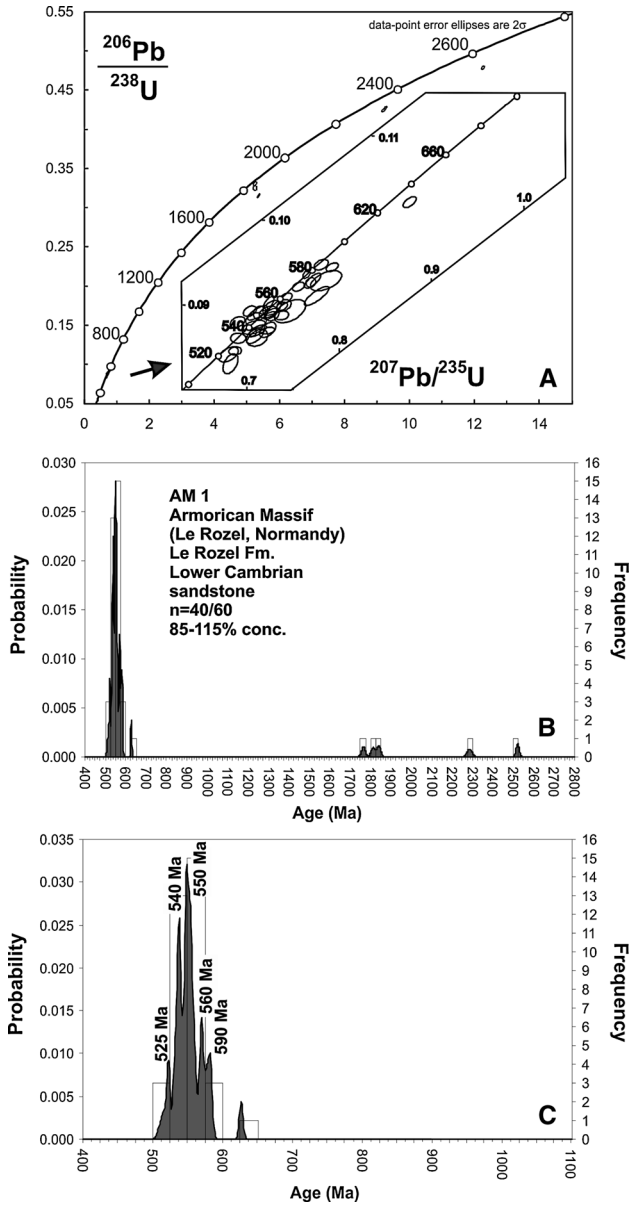

Fig. 7 U–Pb ages of detrital zircon grains from sample AM 1 (sandstone, Lower Cambrian, Le Rozel formation, Le Rozel, Normandy, Armorican Massif). Concordia diagram (**a**) and combined binned frequency and probability density distribution plots of detrital zircon grains in the range of 400–2,900 Ma (**b**) and of 400–1,100 Ma (**c**)

Raw data reduction was performed using LAMTRACE, a macro-based spreadsheet written by Simon Jackson (Macquarie University, Australia). Calculations and plotting of concordia diagrams were achieved using Isoplot/Ex rev. 2.49 (Ludwig 2001), probability density plots and histograms were prepared by AgeDisplay (Sircombe 2004). For grains younger than 1 Ga, the $^{206}Pb/^{238}Pb$ age is quoted. For grains older than 1 Ga, the $^{207}Pb/^{206}Pb$ age is used. Only grains concordant in the range 85–115 % were used in the probability plots and histograms.

Results

U–Pb data of detrital zircon grains are represented in the concordia, histograms and binned frequency plots of Figs. 6, 7, 8, 9, 10 and in the supplementary data Tables 1, 2, 3, 4, 5. The tables also contain information on litho- and biostratigraphy, sample location and co-ordinates.

Sample ROC 1 is dominated by late Neoproterozoic grains (30 out of 48) that lie close to or on concordia and range in age from 547 ± 8 to 685 ± 11 Ma (Fig. 6). Of

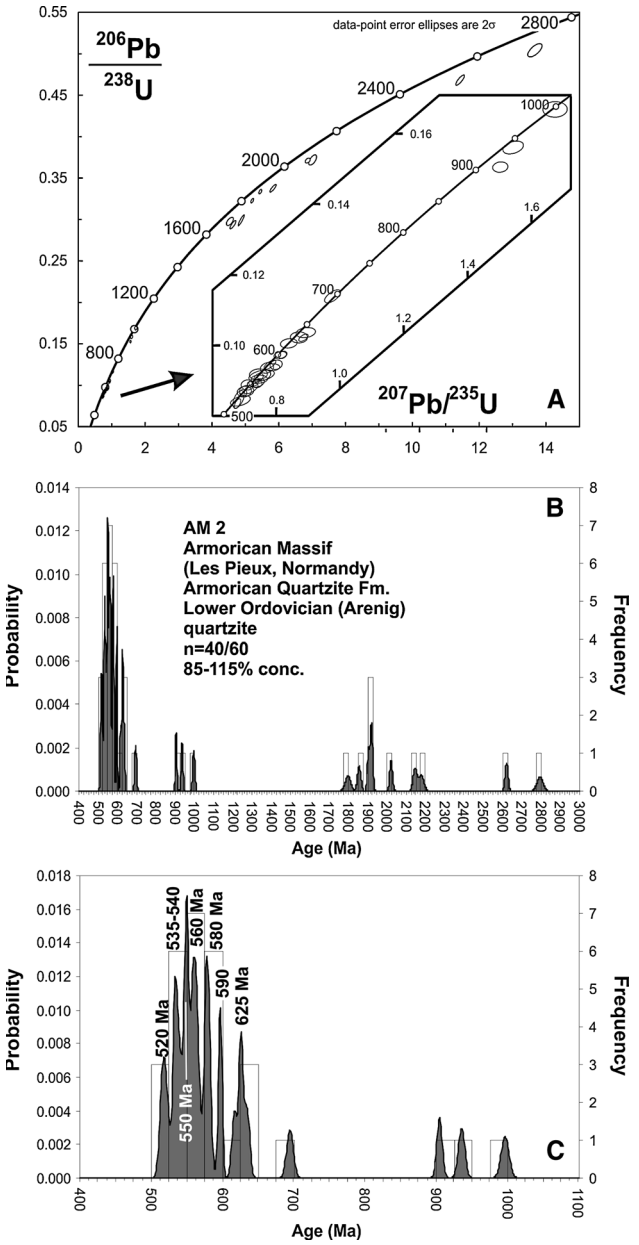

Fig. 8 U–Pb ages of detrital zircon grains from sample AM 2 (quartzite, Lower Ordovician (Arenigian), Armorican quartzite formation, Les Rieux, Normandy, Armorican Massif). Concordia diagram (**a**) and combined binned frequency and probability density distribution plots of detrital zircon grains in the range of 400–3,000 Ma (**b**) and of 400–1,100 Ma (**c**)

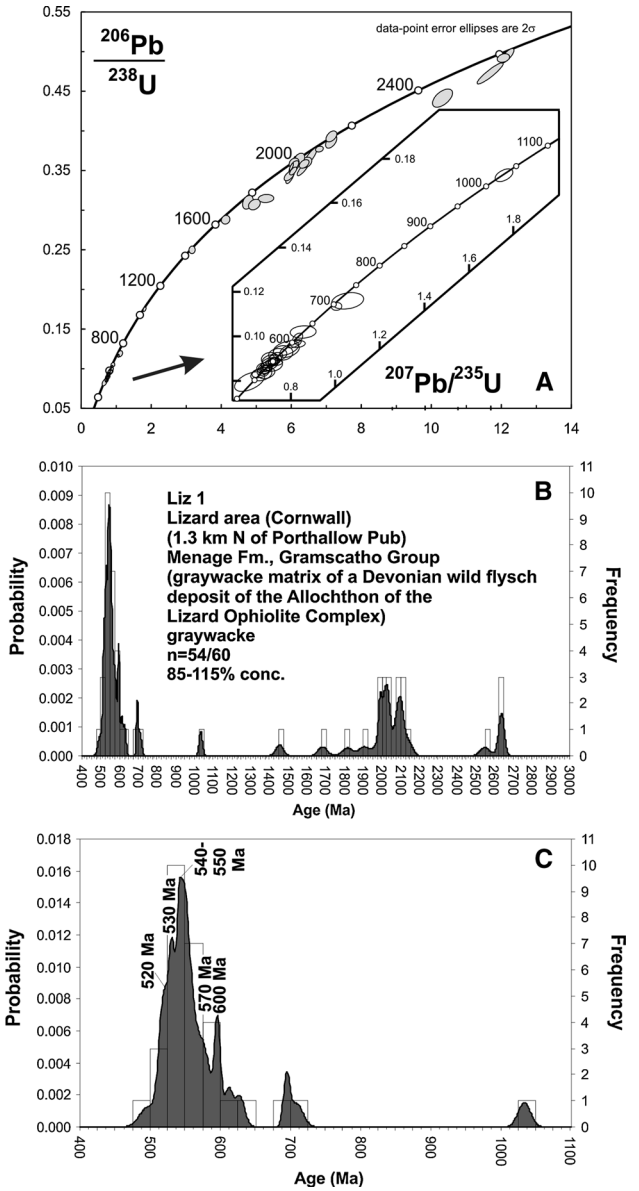

Fig. 9 U–Pb ages of detrital zircon grains from sample LIZ 1 (greywacke matrix of the mélange deposit, Devonian, Meneage Formation, Gramscatho Group, Nare Cove, c. 1.3 km north of Porthallow, Cornwall, UK). Concordia diagram (**a**) and combined binned frequency and probability density distribution plots of detrital zircon grains in the range of 400–3,000 Ma (**b**) and of 400–1,100 Ma (**c**)

the remaining analyses, most are variably discordant. Thirteen yield Palaeoproterozoic ages with relative age peaks of c. 1,850, 2,100 and 2,400 Ma, four are Neoarchaean and the oldest grain is dated at 3,113 ± 31 Ma.

Sample AM 1 is dominated by late Neoproterozoic to early Cambrian grains (35 out of 40) that mostly lie close to or on concordia and range in age from 514 ± 10 to 627 ± 5 Ma (Fig. 7). The remaining five analyses are somewhat discordant. Four Palaeoproterozoic grains yield ages of c. 1,800 Ma(3), c. 2,300 Ma(1), and the oldest grain is latest Neoarchaean and dated at 2,522 ± 15 Ma.

Sample AM 2 is dominated by late Neoproterozoic to middle Cambrian grains (27 out of 40) close to or on concordia and ranging in age from 515 ± 7 to 695 ± 9 Ma (Fig. 8). An older Neoproterozoic cluster features three concordant or slightly discordant analyses at c. 905–997 Ma. Of the remaining ten analyses, nine are

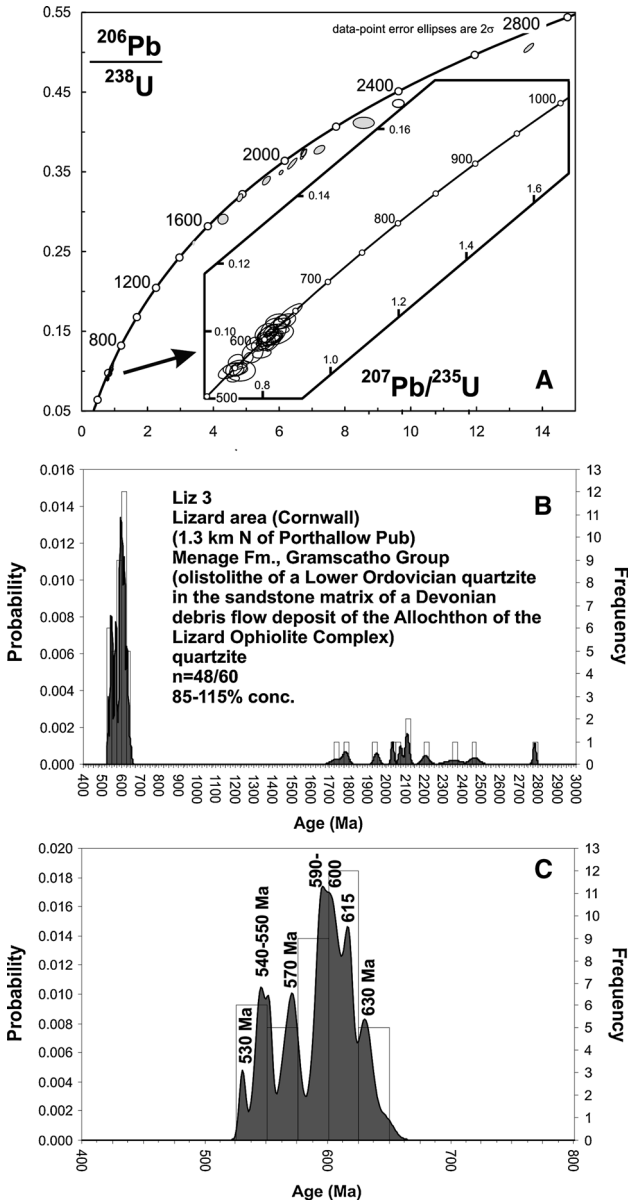

Fig. 10 U–Pb ages of detrital zircon grains from sample LIZ 3 (quartzite olistolith correlated with the Armorican quartzite in the mélange deposit of the Devonian Meneage Formation, Gramscatho Group, Nare Cove, c. 1.3 km north of Porthallow, Cornwall, UK) (see also Fig. 4). Concordia diagram (**a**) and combined binned frequency and probability density distribution plots of detrital zircon grains in the range of 400–3,000 Ma (**b**) and of 400–800 Ma (**c**)

Palaeoproterozoic with relative age peaks of c. 1,800, 1,850, 1,900, 2,000 and 2,150 Ma, and the oldest grain is Neoarchaean and dated at 2,636 ± 35 Ma.

Sample LIZ 1 is dominated by late Neoproterozoic to late Cambrian grains (29 out of 54) close to or on concordia and ranging in age from 496 ± 22 to 709 ± 18 Ma (Fig. 9). Two Mesoproterozoic grains yield ages of c. 1,028 and 1,431 Ma. Of the remaining nineteen analyses, eighteen are Palaeoproterozoic with major relative age peaks at c. 2,000 and 2,100 Ma, and the oldest grain is Neoarchaean and dated at 2,593 ± 39 Ma.

Sample LIZ 3 is dominated by late Neoproterozoic to early Cambrian grains (37 out of 50) close to or on concordia and ranging in age from 531 ± 5 to 646 ± 14 Ma (Fig. 10). Two Mesoproterozoic grains yield ages of c. 1,338 and 1,485 Ma. Of the remaining eleven slightly discordant analyses, ten are Palaeoproterozoic with major relative age peaks at c. 2,000 and 2,100 Ma, and the oldest grain is Neoarchaean and dated at 2,641 ± 25 Ma.

Discussion and conclusions

Detrital zircons analysed from the three samples obtained from the Armorican Massif have a distinctive bimodal age distribution, dominated by late Neoproterozoic to middle Cambrian (c. 710–518 Ma) and Palaeoproterozoic (c. 1,800–2,200 Ma) groupings (Fig. 11). Additionally, the samples contain minor amounts of Mesoproterozoic to early Neoproterozoic detritus. There has been much debate surrounding what is a meaningful statistical population in detrital zircon analysis (e.g. Dodson et al. 1988; Sircombe 2000). According to Dodson et al. (1988), at least 59 randomly selected grains need to be measured to reduce the probability of missing a provenance component to 5 %. In our study, we measured 60 grains per sample, 40–50 of which yielded analyses that were in the range of concordance of 85–115 % and incorporated into data presentation and interpretation. Taking the three Armorican samples together (ROC 1, AM 1 and AM 2), this equates to 127 analyses, and the two Lizard samples (LIZ 1 and LIZ 2) provide a further 104 analyses. We are therefore confident that we have identified all major provenance components within the two sets of samples.

The samples have essentially the same bimodal age distribution as detrital zircons analysed from other samples of the Brioverian Supergroup (Fernández-Suárez et al. 2002b; Samson et al. 2005). Both groupings can be readily linked with lithologies exposed within the Cadomian belt as well as the West African craton which is characterized by major tectonothermal events at 2.0–2.4 Ga (Fig. 11). Similar detrital zircon age distributions are characteristic of Neoproterozoic successions in SW Iberia (Fernández-Suárez et al. 2002a) and, in particular, the Saxothuringian and Moldanubian zones in central Europe (Fig. 11). On this basis, these crustal blocks are thought to have been located adjacent to the NW Africa segment of the Gondwanan margin during the Neoproterozoic and Lower Palaeozoic (Fernández-Suárez et al. 2002b; Samson et al. 2005).

The detrital zircon signature of Avalonia is quite distinct from that of Armorica in that there is a much larger

Table 1 LA-ICP-MS detrital zircon data of sample ROC 1, $n = 48/60$, concordant in the range of 85–115 %, greywacke turbidite from the Upper Brioverian (Post-Bedded Chert Brioverian), Bocaine Zone, Rocreux near Bretteville s. Laize, Normandy, France, (sample location: road cut at Rocreux in the valley of the Laize river, co-ordinates: 49°03′16.03″N, 0°20′41.28″W)

Spot	Grain	206/238	Err	207/235	Err	207/206	Err
mr24h09	ROC1 41	0.08850	0.00070	0.72190	0.01011	0.05914	0.00100
mr24g07	ROC1 27	0.09030	0.00062	0.72920	0.00620	0.05856	0.00042
mr24e13	ROC1 09	0.09080	0.00066	0.72480	0.01348	0.05791	0.00119
mr24k08	ROC1 52	0.09110	0.00055	0.76060	0.00578	0.06051	0.00042
mr24f05	ROC1 13	0.09160	0.00059	0.72960	0.00883	0.05776	0.00077
mr24h11	ROC1 43	0.09200	0.00063	0.73330	0.01085	0.05779	0.00091
mr24f08	ROC1 16	0.09220	0.00069	0.76690	0.00759	0.06029	0.00037
mr24k14	ROC1 58	0.09280	0.00073	0.76530	0.00574	0.05977	0.00057
mr24k15	ROC1 59	0.09290	0.00051	0.76370	0.00672	0.05958	0.00046
mr24f13	ROC1 21	0.09320	0.00072	0.76620	0.00766	0.05960	0.00069
mr24f11	ROC1 19	0.09350	0.00071	0.73680	0.00936	0.05717	0.00065
mr24e16	ROC1 12	0.09370	0.00124	0.78500	0.01256	0.06078	0.00055
mr24e07	ROC1 03	0.09440	0.00048	0.80910	0.00744	0.06213	0.00066
mr24e08	ROC1 04	0.09500	0.00085	0.77010	0.00901	0.05878	0.00045
mr24g14	ROC1 34	0.09510	0.00078	0.77060	0.00709	0.05875	0.00052
mr24f09	ROC1 17	0.09530	0.00055	0.77960	0.00686	0.05935	0.00049
mr24g08	ROC1 28	0.09590	0.00081	0.79630	0.00764	0.06020	0.00034
mr24k12	ROC1 56	0.09600	0.00122	0.78170	0.01610	0.05902	0.00133
mr24k07	ROC1 51	0.09630	0.00120	0.79650	0.01027	0.05999	0.00079
mr24e14	ROC1 10	0.09680	0.00102	0.82690	0.01125	0.06193	0.00048
mr24g10	ROC1 30	0.09880	0.00075	0.81750	0.00891	0.06002	0.00053
mr24h05	ROC1 37	0.09950	0.00086	0.83410	0.00859	0.06079	0.00075
mr24h13	ROC1 45	0.10030	0.00090	0.83620	0.00828	0.06045	0.00073
mr24h10	ROC1 42	0.10080	0.00065	0.84920	0.00977	0.06109	0.00063
mr24h06	ROC1 38	0.10110	0.00086	0.85570	0.00625	0.06139	0.00041
mr24k05	ROC1 49	0.10150	0.00066	0.85330	0.00700	0.06098	0.00035
mr24g06	ROC1 26	0.10320	0.00090	0.87950	0.00774	0.06181	0.00041
mr24g09	ROC1 29	0.10400	0.00063	0.85110	0.02247	0.05933	0.00160
mr24g12	ROC1 32	0.10850	0.00100	0.91260	0.01342	0.06097	0.00098
mr24e06	ROC1 02	0.10870	0.00096	0.92580	0.01120	0.06175	0.00054
mr24f16	ROC1 24	0.11220	0.00096	0.93560	0.01927	0.06049	0.00142
mr24h15	ROC1 47	0.32290	0.00165	5.19900	0.03171	0.11676	0.00077
mr24k16	ROC1 60	0.32830	0.00230	5.69070	0.05065	0.12569	0.00057
mr24f14	ROC1 22	0.33170	0.00226	5.28300	0.03381	0.11550	0.00069
mr24h16	ROC1 48	0.33610	0.00192	5.76650	0.03402	0.12440	0.00049

Table 1 continued

Spot	Grain	206/238	Err	207/235	Err	207/206	Err
mr24f15	ROC1 23	0.33660	0.00293	5.27860	0.06229	0.11372	0.00156
mr24k06	ROC1 50	0.37000	0.00185	6.49950	0.02795	0.12739	0.00059
mr24e12	ROC1 08	0.37550	0.00308	6.77600	0.04608	0.13084	0.00079
mr24h08	ROC1 40	0.38180	0.00191	6.74800	0.04184	0.12814	0.00041
mr24f06	ROC1 14	0.38900	0.00233	7.10970	0.06043	0.13252	0.00091
mr24e05	ROC1 01	0.43810	0.00215	10.24630	0.06148	0.16958	0.00078
mr24k11	ROC1 55	0.45130	0.00420	10.75860	0.10543	0.17287	0.00109
mr24h14	ROC1 46	0.49920	0.00180	14.28570	0.05571	0.20753	0.00114
mr24e10	ROC1 06	0.51990	0.00452	13.14520	0.10385	0.18333	0.00055
mr24h07	ROC1 39	0.54420	0.00332	16.15720	0.10664	0.21530	0.00086
mr24f10	ROC1 18	0.55130	0.00402	15.15010	0.11666	0.19927	0.00145
mr24g15	ROC1 35	0.62090	0.00385	21.50850	0.15916	0.25120	0.00103
Spot	Age 206/238	2σ	Age 207/235	2σ	Age 207/206	2σ	Conc %
mr24h09	547	8	552	12	572	74	96
mr24g07	557	7	556	7	550	32	101
mr24e13	560	8	554	16	526	90	106
mr24k08	562	6	574	7	622	30	90
mr24f05	565	7	556	10	520	58	109
mr24h11	567	7	558	13	520	68	109
mr24f08	569	8	578	9	612	26	93
mr24k14	572	9	577	7	594	42	96
mr24k15	573	6	576	8	588	34	97
mr24f13	575	9	578	9	588	52	98
mr24f11	576	8	561	11	498	50	116
mr24e16	577	15	588	14	630	40	92
mr24e07	582	6	602	8	678	46	86
mr24e08	585	10	580	10	558	32	105
mr24g14	586	9	580	8	556	38	105
mr24f09	587	7	585	8	578	36	102
mr24g08	590	9	595	9	610	24	97
mr24k12	591	14	586	18	566	100	104
mr24k07	592	14	595	12	602	56	98
mr24e14	596	12	612	13	670	34	89
mr24g10	607	9	607	10	604	38	100

Table 1 continued

Spot	Age 206/238	2σ	Age 207/235	2σ	Age 207/206	2σ	Conc %
mr24h05	611	10	616	9	630	52	97
mr24h13	616	11	617	9	618	52	100
mr24h10	619	8	624	11	642	44	96
mr24h06	621	10	628	7	652	28	95
mr24k05	623	8	626	8	638	24	98
mr24g06	633	10	641	8	666	28	95
mr24g09	638	7	625	25	578	118	110
mr24g12	664	12	658	14	638	70	104
mr24e06	665	11	665	12	664	38	100
mr24f16	685	11	671	20	620	102	110
mr24h15	1,804	16	1,852	10	1,906	24	95
mr24k16	1,830	22	1,930	15	2,038	16	90
mr24f14	1,847	22	1,866	11	1,886	22	98
mr24h16	1,868	19	1,941	10	2,020	14	92
mr24f15	1,870	28	1,865	20	1,858	50	101
mr24k06	2,029	17	2,046	7	2,062	16	98
mr24e12	2,055	29	2,083	12	2,108	20	97
mr24h08	2,085	18	2,079	11	2,072	12	101
mr24f06	2,118	22	2,125	15	2,130	24	99
mr24e05	2,342	19	2,457	11	2,552	16	92
mr24k11	2,401	37	2,502	18	2,584	22	93
mr24h14	2,610	15	2,769	7	2,886	18	90
mr24e10	2,699	38	2,690	15	2,682	10	101
mr24h07	2,801	28	2,886	13	2,944	14	95
mr24f10	2,831	33	2,825	15	2,820	24	100
mr24g15	3,113	31	3,162	14	3,192	14	98

Table 2 LA-ICP-MS detrital zircon data for sample AM 1, $n = 40/60$, concordant in the range of 85–115 %, quartzite from the Le Rozel Formation, Lower Cambrian, Normandy, Armorican Massif, France (sample location: beach south of Le Rozel, co-ordinates: 49°28′46″N, 01°50′39″W)

Spot	Grain	206/238	Err	207/235	Err	207/206	Err
mr18b16	AM1-48	0.08310	0.0008	0.6821	0.00539	0.05953	0.00054
mr18c08	AM1-52	0.08420	0.0006	0.6800	0.00700	0.05855	0.00054
mr18c11	AM1-55	0.08460	0.0003	0.6871	0.00467	0.05891	0.00043
mr17g06	AM1-2	0.08610	0.0004	0.6904	0.00545	0.05816	0.00054
mr18b13	AM1-45	0.08620	0.0007	0.7109	0.00768	0.05980	0.00070
mr18a05	AM1-25	0.08630	0.0006	0.7089	0.00595	0.05955	0.00038
mr17g05	AM1-1	0.08680	0.0004	0.7026	0.00499	0.05870	0.00047
mr18a11	AM1-31	0.08700	0.0004	0.7116	0.00626	0.05927	0.00040
mr18b10	AM1-42	0.08700	0.0003	0.7225	0.00506	0.06023	0.00039
mr17h09	AM1-17	0.08710	0.0006	0.7224	0.00592	0.06011	0.00045
mr18c14	AM1-58	0.08740	0.0006	0.7075	0.00849	0.05872	0.00063
mr17h07	AM1-15	0.08800	0.0004	0.6896	0.00531	0.05679	0.00041
mr17g10	AM1-6	0.08820	0.0006	0.7099	0.00738	0.05839	0.00076
mr18b14	AM1-46	0.08880	0.0003	0.7378	0.00494	0.06025	0.00043
mr18c07	AM1-51	0.08880	0.0003	0.7249	0.00457	0.05920	0.00028
mr18b06	AM1-38	0.08890	0.0005	0.7276	0.00466	0.05937	0.00042
mr17h14	AM1-22	0.08910	0.0006	0.7116	0.00726	0.05793	0.00039
mr18a12	AM1-32	0.08910	0.0005	0.7138	0.00450	0.05808	0.00054
mr18a13	AM1-33	0.08930	0.0009	0.7466	0.01127	0.06065	0.00081
mr18b11	AM1-43	0.08920	0.0005	0.7230	0.00636	0.05880	0.00047
mr17h15	AM1-23	0.08930	0.0004	0.7031	0.00464	0.05707	0.00037
mr17g07	AM1-3	0.08970	0.0006	0.7270	0.00654	0.05877	0.00049
mr17h06	AM1-14	0.09000	0.0004	0.7402	0.00496	0.05965	0.00042
mr18a06	AM1-26	0.08990	0.0003	0.7382	0.00384	0.05954	0.00031
mr17h11	AM1-19	0.09020	0.0006	0.7233	0.00383	0.05816	0.00028
mr17g11	AM1-7	0.09080	0.0004	0.7415	0.00482	0.05925	0.00034
mr17h10	AM1-18	0.09110	0.0007	0.7756	0.00884	0.06174	0.00041
mr18b05	AM1-37	0.09220	0.0004	0.7558	0.00431	0.05944	0.00032
mr18b12	AM1-44	0.09270	0.0004	0.7694	0.00354	0.06018	0.00033
mr18b07	AM1-39	0.09290	0.0008	0.7858	0.01116	0.06136	0.00075
mr17g14	AM1-10	0.09290	0.0006	0.7714	0.00586	0.06022	0.00031
mr18a09	AM1-29	0.09370	0.0004	0.7649	0.00283	0.05918	0.00021
mr18a10	AM1-30	0.09450	0.0003	0.7924	0.00428	0.06077	0.00030
mr18c16	AM1-60	0.09480	0.0004	0.7806	0.00500	0.05973	0.00036
mr18a07	AM1-27	0.10220	0.0004	0.8767	0.00473	0.06220	0.00027
mr17g13	AM1-9	0.31510	0.0017	5.3598	0.02733	0.12334	0.00030
mr17h05	AM1-13	0.32510	0.0019	5.2425	0.03827	0.11694	0.00106
mr17h12	AM1-20	0.33070	0.0017	5.2541	0.03625	0.11520	0.00065
mr18b08	AM1-40	0.42570	0.0023	9.2282	0.05352	0.15719	0.00041
mr17g16	AM1-12	0.47880	0.0014	12.2659	0.03066	0.18577	0.00046

Spot	Age 206/238	2σ	Age 207/235	2σ	Age 207/206	2σ	Conc %
mr18b16	514	10	528	8	586	11	88
mr18c08	521	7	527	11	550	10	95
mr18c11	523	4	531	7	562	8	93
mr17g06	532	5	533	8	534	10	100
mr18b13	533	8	545	12	596	14	89

Table 2 continued

Spot	Age 206/238	2σ	Age 207/235	2σ	Age 207/206	2σ	Conc %
mr18a05	534	7	544	9	586	7	91
mr17g05	537	4	540	8	554	9	97
mr18a11	538	5	546	10	576	8	93
mr18b10	538	3	552	8	610	8	88
mr17h09	539	7	552	9	606	9	89
mr18c14	540	7	543	13	556	12	97
mr17h07	544	5	533	8	482	7	113
mr17g10	545	7	545	11	544	14	100
mr18b14	548	4	561	8	612	9	90
mr18c07	548	4	554	7	574	5	95
mr18b06	549	6	555	7	580	8	95
mr17h14	550	7	546	11	526	7	105
mr18a12	550	6	547	7	532	10	103
mr18a13	551	11	566	17	626	17	88
mr18b11	551	6	552	10	558	9	99
mr17h15	552	5	541	7	494	6	112
mr17g07	554	7	555	10	558	9	99
mr17h06	555	5	563	8	590	8	94
mr18a06	555	4	561	6	586	6	95
mr17h11	557	7	553	6	534	5	104
mr17g11	560	5	563	7	576	7	97
mr17h10	562	9	583	13	664	9	85
mr18b05	569	4	572	7	582	6	98
mr18b12	571	5	579	5	610	7	94
mr18b07	572	10	589	17	650	16	88
mr17g14	573	7	581	9	610	6	94
mr18a09	578	4	577	4	572	4	101
mr18a10	582	4	593	6	630	6	92
mr18c16	584	5	586	8	592	7	99
mr18a07	627	5	639	7	680	6	92
mr17g13	1,766	19	1,878	19	2,004	10	88
mr17h05	1,814	21	1,860	27	1,908	35	95
mr17h12	1,842	18	1,861	26	1,882	21	98
mr18b08	2,286	25	2,361	27	2,424	13	94
mr17g16	2,522	15	2,625	13	2,704	14	93

proportion of Mesoproterozoic detritus (Fig. 11; Collins and Buchan 2004; Murphy et al. 2004; Samson et al. 2005; Strachan et al. 2007). This contrasting signature is consistent with a location close to the Amazonian craton which records Mesoproterozoic tectonothermal activity at c. 1.6 and 1.1 Ga (Murphy et al. 2004; Collins and Buchan 2004; Samson et al. 2005; Strachan et al. 2007). Similar detrital zircon age distributions are characteristic of Neoproterozoic successions in NW Iberia (Fernández-Suárez et al. 2002b) and Bohemia (Friedl et al. 2000; Samson et al. 2005), and by implication these crustal blocks are also thought to have been located adjacent to Amazonia. It has been suggested that a major phase of Cambrian(?) sinistral strike-slip faulting displaced these crustal blocks along the Gondwanan margin into a location between the West African craton and Armorica (Fernández-Suárez et al. 2002b).

The two samples taken from the Devonian Meneage Formation in the footwall of the Lizard ophiolite display an identical provenance to the three samples analysed from Armorica (Fig. 11). This is consistent with: (a) the derivation of these mélange deposits from the over-riding Armorican plate during closure of the Rheic Ocean, collision of Avalonia and Armorica, and obduction of the

Table 3 LA-ICP-MS detrital zircon data for sample AM 2, $n = 39/60$, concordant in the range of 85–115 %, quartzite from the Armorican Quartzite Formation, Lower Ordovician (Arenig), Normandy, Armorican Massif, France (sample location: c. 2 km SW of the city of Les Pieux; co-ordinates: 49°30′26″N, 1°50′21″W)

Spot	Grain	206/238	Err	207/235	Err	207/206	Err
mr17f05	AM2-49	0.08320	0.00058	0.67430	0.00418	0.058800	0.000329
mr17f13	AM2-57	0.08400	0.00060	0.68390	0.01265	0.059010	0.000974
mr17c16	AM2-24	0.08440	0.00104	0.67820	0.00732	0.058240	0.000641
mr17f06	AM2-50	0.08630	0.00040	0.69280	0.00478	0.058230	0.000466
mr17f16	AM2-60	0.08660	0.00062	0.69610	0.00912	0.058290	0.000816
mr17d13	AM2-33	0.08690	0.00061	0.70290	0.00907	0.058650	0.000886
mr17b12	AM2-8	0.08750	0.00060	0.71730	0.00861	0.059430	0.001022
mr17e05	AM2-37	0.08850	0.00059	0.70560	0.00804	0.057830	0.000746
mr17f10	AM2-54	0.08880	0.00045	0.73510	0.00654	0.060010	0.000588
mr17e10	AM2-42	0.08910	0.00048	0.73970	0.00814	0.060190	0.000620
mr17b11	AM2-7	0.08920	0.00043	0.72480	0.00623	0.058890	0.000536
mr17e06	AM2-38	0.09020	0.00048	0.74290	0.01047	0.059700	0.000907
mr17b07	AM2-3	0.09060	0.00053	0.74050	0.00622	0.059260	0.000486
mr17b14	AM2-10	0.09130	0.00061	0.75780	0.00849	0.060210	0.000668
mr17e12	AM2-44	0.09120	0.00067	0.74980	0.01635	0.059620	0.001175
mr17d07	AM2-27	0.09160	0.00062	0.74060	0.01163	0.058650	0.001044
mr17c14	AM2-22	0.09340	0.00062	0.76730	0.00867	0.059580	0.000697
mr17f08	AM2-52	0.09360	0.00041	0.78410	0.00917	0.060730	0.000783
mr17b09	AM2-5	0.09430	0.00054	0.77620	0.00768	0.059700	0.000424
mr17e09	AM2-41	0.09430	0.00055	0.79570	0.00780	0.061160	0.000636
mr17e08	AM2-40	0.09710	0.00043	0.81630	0.00555	0.060960	0.000421
mr17f09	AM2-53	0.09700	0.00043	0.80860	0.00809	0.060430	0.000586
mr17b13	AM2-9	0.10040	0.00056	0.83580	0.01078	0.060390	0.000791
mr17d14	AM2-34	0.10200	0.00042	0.88220	0.00618	0.062710	0.000357
mr17f12	AM2-56	0.10210	0.00065	0.86760	0.01085	0.061590	0.000856
mr17b16	AM2-12	0.10350	0.00059	0.88920	0.01263	0.062330	0.000885
mr17b15	AM2-11	0.11380	0.00077	0.97380	0.01032	0.062060	0.000503
mr17e15	AM2-47	0.15070	0.00062	1.50140	0.00976	0.072230	0.000527
mr17e11	AM2-43	0.15630	0.00075	1.54170	0.01310	0.071500	0.000579
mr17c06	AM2-14	0.16720	0.00090	1.67390	0.01557	0.072580	0.000769
mr17f15	AM2-59	0.29290	0.00205	4.58910	0.03855	0.113610	0.000534
mr17e07	AM2-39	0.29700	0.00196	4.50310	0.04368	0.109930	0.000846
mr17b05	AM2-1	0.32210	0.00110	5.17950	0.01813	0.116590	0.000326
mr17b05	AM2-1	0.32210	0.00110	5.17950	0.01813	0.116590	0.000326
mr17c08	AM2-16	0.33340	0.00110	5.41160	0.01840	0.117710	0.000377
mr17e13	AM2-45	0.33720	0.00189	5.79330	0.03824	0.124590	0.000436
mr17f11	AM2-55	0.37090	0.00126	6.83810	0.03214	0.133670	0.000615
mr17e16	AM2-48	0.37170	0.00253	6.98300	0.04958	0.136210	0.000858
mr17c12	AM2-20	0.46860	0.00253	11.42780	0.05143	0.176860	0.000513
mr17c11	AM2-19	0.50520	0.00333	13.67910	0.08891	0.196360	0.001060

Spot	Age 206/238	2σ	Age 207/235	2σ	Age 207/206	2σ	Conc %
mr17f05	515	7	523	6	558	6.2	92
mr17f13	520	7	529	20	566	18.7	92
mr17c16	523	13	526	11	538	11.8	97
mr17f06	533	5	534	7	538	8.6	99
mr17f16	535	8	536	14	540	15.1	99

Table 3 continued

Spot	Age 206/238	2σ	Age 207/235	2σ	Age 207/206	2σ	Conc %
mr17d13	537	8	541	14	552	16.7	97
mr17b12	541	7	549	13	582	20.0	93
mr17e05	547	7	542	12	522	13.5	105
mr17f10	549	6	560	10	604	11.8	91
mr17e10	550	6	562	12	610	12.6	90
mr17b11	551	5	553	10	562	10.2	98
mr17e06	557	6	564	16	592	18.0	94
mr17b07	559	6	563	9	576	9.4	97
mr17b14	563	8	573	13	610	13.5	92
mr17e12	563	8	568	25	588	23.2	96
mr17d07	565	8	563	18	554	19.7	102
mr17c14	576	8	578	13	588	13.8	98
mr17f08	577	5	588	14	628	16.2	92
mr17b09	581	7	583	12	592	8.4	98
mr17e09	581	7	594	12	644	13.4	90
mr17e08	597	5	606	8	636	8.8	94
mr17f09	597	5	602	12	618	12.0	97
mr17b13	617	7	617	16	616	16.1	100
mr17d14	626	5	642	9	698	8.0	90
mr17f12	627	8	634	16	658	18.3	95
mr17b16	635	7	646	18	684	19.4	93
mr17b15	695	9	690	15	676	11.0	103
mr17e15	905	7	931	12	992	14.5	91
mr17e11	936	9	947	16	970	15.7	96
mr17c06	997	11	999	19	1,002	21.2	100
mr17f15	1,656	23	1,747	29	1,856	17.4	89
mr17e07	1,676	22	1,732	34	1,798	27.7	93
mr17b05	1,800	12	1,849	13	1,904	10.7	95
mr17b05	1,800	12	1,849	13	1,904	10.7	95
mr17c08	1,855	12	1,887	13	1,920	12.3	97
mr17e13	1,873	21	1,945	26	2,022	14.2	93
mr17f11	2,034	14	2,091	20	2,146	19.7	95
mr17e16	2,038	28	2,109	30	2,178	27.4	94
mr17c12	2,477	27	2,559	23	2,622	15.2	94
mr17c11	2,636	35	2,728	35	2,796	30.2	94

Lizard ophiolite (Fig. 12; Holder and Leveridge 1986; Dörr et al. 1999) and (b) the correlation of the quartzite blocks within the Meneage Formation with the Ordovician Grès Armoricain Formation (Sadler 1974). The absence of identifiable clasts of Brioverian material in the Meneage Formation suggests that many of the detrital zircons are second cycle, derived from reworking of the Lower Palaeozoic cover to the basement of Armorica. We cannot absolutely preclude the incorporation of Avalonian material within the Meneage Formation, and further material needs to be analysed to provide a broader database. The presence of two Mesoproterozoic grains within sample LIZ 1 might be taken as indicative of at least partial derivation from an Avalonian source. However, sample LIZ 3 also contains two Mesoproterozoic grains but is more firmly linked to Armorica by the palaeontological evidence (Sadler 1974).

Our data set is therefore consistent with the south-directed subduction geometry of the Rheic collision zone invoked by Holder and Leveridge (1986) (Fig. 12). Such a geometry would be expected to have resulted in the generation of a magmatic arc on the over-riding Armorican plate, consistent with the Silurian-Devonian U–Pb zircon ages obtained from granite pebbles in the Meneage

Table 4 LA-ICP-MS detrital zircon data of sample LIZ 1, $n = 54/60$, concordant in the range of 85–115 %, a sandstone from the matrix of the Meneage Formation, Gramscatho Group, age of sedimentation is Devonian, Cornwall, Great Britain (sample location: c. 1.3 km north of Porthallow, co-ordinates: 50°04′40″N, 5°04′37″W)

Spot	Grain	206/238	Err	207/235	Err	207/206	Err
mr29g11	LIZ1 43	0.08	0.0018	0.6141	0.027512	0.05567	0.002138
mr29g09	LIZ1 41	0.0833	0.001208	0.667	0.019343	0.05805	0.002078
mr29f11	LIZ1 31	0.0837	0.000795	0.6625	0.01537	0.05737	0.001279
mr29g07	LIZ1 39	0.0837	0.000988	0.6912	0.01493	0.05986	0.00167
mr29f12	LIZ1 32	0.085	0.000918	0.6769	0.011575	0.05777	0.001369
mr30a14	LIZ1 60	0.0856	0.00083	0.6888	0.009988	0.05835	0.000776
mr29d14	LIZ1 10	0.08600	0.0006	0.6843	0.00876	0.05773	0.00088
mr29e14	LIZ1 22	0.08600	0.0010	0.6811	0.01430	0.05739	0.00141
mr29f06	LIZ1 26	0.0871	0.001028	0.6982	0.018083	0.05811	0.00129
mr30a16	LIZ1 62	0.0876	0.000517	0.7156	0.006655	0.05923	0.000432
mr29d05	LIZ1 01	0.08770	0.0012	0.7148	0.01930	0.05911	0.00186
mr29e10	LIZ1 18	0.08780	0.0006	0.6988	0.01412	0.05773	0.00137
mr29e13	LIZ1 21	0.08860	0.0006	0.7240	0.01600	0.05924	0.00134
mr29d15	LIZ1 11	0.08900	0.0007	0.7245	0.01101	0.05905	0.00089
mr29f10	LIZ1 30	0.0893	0.000688	0.7234	0.010128	0.05875	0.000852
mr29g08	LIZ1 40	0.0896	0.000995	0.7048	0.014166	0.05704	0.001112
mr29e09	LIZ1 17	0.09010	0.0012	0.7059	0.01574	0.05682	0.00144
mr30a05	LIZ1 51	0.0902	0.00074	0.7283	0.012308	0.05857	0.001066
mr29e15	LIZ1 23	0.09110	0.0008	0.7341	0.01175	0.05840	0.00095
mr29f08	LIZ1 28	0.0922	0.001097	0.7407	0.016814	0.05822	0.001572
mr29f07	LIZ1 27	0.0929	0.001338	0.7641	0.018262	0.05966	0.001617
mr29g16	LIZ1 48	0.0939	0.001249	0.7939	0.01818	0.06133	0.001257
mr29h05	LIZ1 49	0.095	0.001349	0.7777	0.023331	0.05935	0.001608
mr30a08	LIZ1 54	0.0969	0.00064	0.8308	0.013791	0.06216	0.001044
mr30a09	LIZ1 55	0.097	0.000766	0.8156	0.012805	0.06095	0.000768
mr30a11	LIZ1 57	0.0995	0.000935	0.8305	0.009385	0.06052	0.000684
mr29e16	LIZ1 24	0.10230	0.0011	0.8550	0.02377	0.06061	0.00176
mr29e17	LIZ1 25	1.10230	1.0011	1.8550	1.02377	1.06061	1.00176
mr30a10	LIZ1 56	0.1138	0.000728	1.0052	0.00975	0.06406	0.000724
mr29e05	LIZ1 13	0.11630	0.0015	1.0551	0.02944	0.06579	0.00220
mr29g05	LIZ1 37	0.1728	0.001158	1.7577	0.016347	0.07375	0.00062
mr29d08	LIZ1 04	0.24850	0.0019	3.1318	0.03602	0.09137	0.00124
mr29f15	LIZ1 35	0.2867	0.002322	4.0855	0.052294	0.10332	0.001467
mr29g10	LIZ1 42	0.306	0.002815	4.9147	0.065857	0.11646	0.001607
mr29d09	LIZ1 05	0.30900	0.0036	4.7309	0.06434	0.11102	0.00167
mr29f09	LIZ1 29	0.3138	0.002071	5.2531	0.091404	0.1214	0.002319
mr29e08	LIZ1 16	0.34270	0.0026	5.9168	0.05917	0.12518	0.00101
mr29e06	LIZ1 14	0.34330	0.0043	5.9428	0.05467	0.12552	0.00113
mr29d10	LIZ1 06	0.34880	0.0020	6.0279	0.04280	0.12530	0.00070
mr30a15	LIZ1 61	0.3518	0.003764	6.3153	0.069468	0.13018	0.000794
mr29f14	LIZ1 34	0.3533	0.002473	6.0581	0.061793	0.12432	0.000982
mr29d12	LIZ1 08	0.35410	0.0019	5.9738	0.02330	0.12233	0.00045
mr29e07	LIZ1 15	0.35580	0.0025	6.0685	0.04794	0.12367	0.00088
mr29g13	LIZ1 45	0.3579	0.002219	6.3404	0.05643	0.12845	0.001066
mr29d13	LIZ1 09	0.35880	0.0025	6.0575	0.05997	0.12243	0.00132
mr29g12	LIZ1 44	0.3596	0.002805	6.401	0.06593	0.12907	0.001394
mr30a12	LIZ1 58	0.3656	0.005374	6.5054	0.088473	0.12901	0.000864
mr29d11	LIZ1 07	0.37670	0.0016	6.7777	0.04406	0.13047	0.00091
mr29f16	LIZ1 36	0.3862	0.003399	7.1264	0.065563	0.13379	0.001191
mr29d16	LIZ1 12	0.39280	0.0028	7.1248	0.06341	0.13152	0.00112
mr29g15	LIZ1 47	0.4415	0.004636	10.3124	0.117561	0.16937	0.001728

Table 4 continued

Spot	Grain	206/238	Err	207/235	Err	207/206	Err
mr30a13	LIZ1 59	0.4729	0.00558	11.6886	0.149614	0.17922	0.000914
mr29d06	LIZ1 02	0.49230	0.0022	12.0694	0.07121	0.17777	0.00114
mr29h06	LIZ1 50	0.4952	0.003764	12.1739	0.080348	0.17827	0.000874
Spot	Age 206/238	2σ	Age 207/235	2σ	Age 207/206	2σ	Conc %
mr29g11	496	22	486	44	438	34	113
mr29g09	516	15	519	30	530	38	97
mr29f11	518	10	516	24	504	22	103
mr29g07	518	12	534	23	598	33	87
mr29f12	526	11	525	18	520	25	101
mr30a14	529	10	532	15	542	14	98
mr29d14	532	8	529	14	518	16	103
mr29e14	532	12	527	22	506	25	105
mr29f06	538	13	538	28	532	24	101
mr30a16	541	6	548	10	574	8	94
mr29d05	542	15	548	30	570	36	95
mr29e10	542	7	538	22	518	25	105
mr29e13	547	7	553	24	574	26	95
mr29d15	549	9	553	17	568	17	97
mr29f10	551	8	553	15	556	16	99
mr29g08	553	12	542	22	492	19	112
mr29e09	556	15	542	24	484	25	115
mr30a05	556	9	556	19	550	20	101
mr29e15	562	10	559	18	544	18	103
mr29f08	569	14	563	26	538	29	106
mr29f07	573	17	576	28	590	32	97
mr29g16	578	15	593	27	650	27	89
mr29h05	585	17	584	35	580	31	101
mr30a08	596	8	614	20	678	23	88
mr30a09	597	9	606	19	636	16	94
mr30a11	612	12	614	14	622	14	98
mr29e16	628	14	627	35	624	36	101
mr29e17	629	15	628	36	625	37	102
mr30a10	695	9	706	14	742	17	94
mr29e05	709	18	731	41	798	53	89
mr29g05	1,028	14	1,030	19	1,034	17	99
mr29d08	1,431	21	1,441	33	1,454	40	98
mr29f15	1,625	26	1,651	42	1,684	48	96
mr29g10	1,721	32	1,805	48	1,902	52	90
mr29d09	1,736	40	1,773	48	1,816	54	96
mr29f09	1,759	23	1,861	65	1,976	75	89
mr29e08	1,900	29	1,964	39	2,030	33	94
mr29e06	1,903	48	1,968	36	2,036	37	93
mr29d10	1,929	22	1,980	28	2,032	23	95
mr30a15	1,943	42	2,021	44	2,100	26	93
mr29f14	1,950	27	1,984	40	2,018	32	97
mr29d12	1,954	21	1,972	15	1,990	15	98
mr29e07	1,962	27	1,986	31	2,008	29	98
mr29g13	1,972	24	2,024	36	2,076	34	95
mr29d13	1,976	28	1,984	39	1,992	43	99
mr29g12	1,980	31	2,032	42	2,084	45	95
mr30a12	2,009	59	2,047	56	2,084	28	96

Table 4 continued

Spot	Age 206/238	2σ	Age 207/235	2σ	Age 207/206	2σ	Conc %
mr29d11	2,061	17	2,083	27	2,104	29	98
mr29f16	2,105	37	2,127	39	2,148	38	98
mr29d16	2,136	30	2,127	38	2,118	36	101
mr29g15	2,357	49	2,463	56	2,550	52	92
mr30a13	2,496	59	2,580	66	2,644	27	94
mr29d06	2,581	23	2,610	31	2,632	34	98
mr29h06	2,593	39	2,618	35	2,636	26	98

Table 5 LA-ICP-MS detrital zircon data for sample LIZ 3, $n = 50/60$, concordant in the range of 85–115 %, a Lower Ordovician quartzite block in the Meneage Formation, Gramscatho group, age of sedimentation is Devonian, Cornwall, Great Britain (sample location c. 1.3 km north of Porthallow, co-ordinates: 50°04′41″N, 5°04′40″W)

Spot	Grain	206/238	Err	207/235	Err	207/206	Err
mr30f10	LIZ3 54	0.08590	0.00040	0.71400	0.00743	0.06029	0.00065
mr30f08	LIZ3 52	0.08820	0.00052	0.72960	0.00635	0.05996	0.00050
mr30f13	LIZ3 57	0.08830	0.00126	0.73510	0.01779	0.06036	0.00171
mr30e16	LIZ3 48	0.08830	0.00097	0.70520	0.01446	0.05788	0.00100
mr30c11	LIZ3 19	0.08870	0.00084	0.72840	0.01042	0.05955	0.00082
mr30f11	LIZ3 55	0.08870	0.00073	0.71990	0.01476	0.05882	0.00126
mr30e05	LIZ3 37	0.08960	0.00037	0.73040	0.00993	0.05912	0.00073
mr30e09	LIZ3 41	0.09130	0.00075	0.72060	0.00894	0.05725	0.00071
mr30f09	LIZ3 53	0.09200	0.00069	0.75780	0.00599	0.05972	0.00053
mr30b10	LIZ3 06	0.09220	0.00065	0.74940	0.00794	0.05892	0.00071
mr30b12	LIZ3 08	0.09280	0.00049	0.78390	0.01121	0.06123	0.00097
mr30f12	LIZ3 56	0.09340	0.00056	0.79770	0.01125	0.06192	0.00104
mr30d08	LIZ3 28	0.09360	0.00122	0.77050	0.01264	0.05968	0.00113
mr30d11	LIZ3 31	0.09590	0.00074	0.78980	0.00940	0.05971	0.00077
mr30b14	LIZ3 10	0.09630	0.00079	0.77500	0.00922	0.05834	0.00075
mr30c12	LIZ3 20	0.09660	0.00046	0.81670	0.00604	0.06131	0.00045
mr30c05	LIZ3 13	0.09680	0.00103	0.81010	0.01118	0.06069	0.00098
mr30c10	LIZ3 18	0.09710	0.00123	0.83480	0.01052	0.06235	0.00054
mr30f06	LIZ3 50	0.09700	0.00085	0.80660	0.00807	0.06027	0.00080
mr30e11	LIZ3 43	0.09720	0.00068	0.81540	0.01402	0.06083	0.00086
mr30b09	LIZ3 05	0.09750	0.00098	0.81420	0.00814	0.06053	0.00045
mr30f15	LIZ3 59	0.09790	0.00083	0.82570	0.01148	0.06116	0.00077
mr30b13	LIZ3 09	0.09830	0.00065	0.81790	0.01325	0.06035	0.00101
mr30e15	LIZ3 47	0.09870	0.00083	0.83280	0.00974	0.06120	0.00085
mr30e12	LIZ3 44	0.09900	0.00130	0.83710	0.02202	0.06134	0.00202
mr30c07	LIZ3 15	0.09910	0.00095	0.82400	0.00923	0.06030	0.00056
mr30c08	LIZ3 16	0.09920	0.00117	0.81500	0.01190	0.05956	0.00075
mr30d14	LIZ3 34	0.09960	0.00110	0.80720	0.01203	0.05874	0.00089
mr30f05	LIZ3 49	0.10000	0.00160	0.83160	0.01547	0.06028	0.00128
mr30b11	LIZ3 07	0.10030	0.00055	0.85190	0.00912	0.06159	0.00070
mr30e13	LIZ3 45	0.10040	0.00069	0.82380	0.00865	0.05948	0.00049
mr30c14	LIZ3 22	0.10050	0.00045	0.85430	0.00991	0.06161	0.00076
mr30d06	LIZ3 26	0.10220	0.00069	0.85170	0.01243	0.06044	0.00080
mr30d10	LIZ3 30	0.10280	0.00081	0.85560	0.00992	0.06038	0.00073
mr30e06	LIZ3 38	0.10300	0.00090	0.86520	0.01324	0.06091	0.00088
mr30e14	LIZ3 46	0.10320	0.00080	0.83960	0.01259	0.05898	0.00084
mr30d16	LIZ3 36	0.10550	0.00111	0.88190	0.01429	0.06063	0.00061
mr30b08	LIZ3 04	0.23070	0.00134	3.03080	0.01970	0.09527	0.00048

Table 5 continued

Spot	Grain	206/238	Err	207/235	Err	207/206	Err
mr30e10	LIZ3 42	0.25900	0.00137	3.36180	0.01883	0.09411	0.00062
mr30f07	LIZ3 51	0.28960	0.00252	4.25610	0.06469	0.10658	0.00175
mr30d09	LIZ3 29	0.31670	0.00200	4.76850	0.03719	0.10919	0.00083
mr30d15	LIZ3 35	0.33840	0.00220	5.57540	0.04962	0.11947	0.00084
mr30e07	LIZ3 39	0.34860	0.00108	6.02620	0.02410	0.12535	0.00043
mr30c09	LIZ3 17	0.35990	0.00281	6.36850	0.05732	0.12832	0.00053
mr30b07	LIZ3 03	0.36980	0.00203	6.69010	0.03479	0.13118	0.00072
mr30d05	LIZ3 25	0.37190	0.00271	6.71230	0.03759	0.13088	0.00052
mr30d13	LIZ3 33	0.37740	0.00226	7.20060	0.06913	0.13836	0.00116
mr30f16	LIZ3 60	0.41140	0.00288	8.55520	0.13175	0.15080	0.00256
mr30b05	LIZ3 01	0.43290	0.00212	9.62040	0.07504	0.16114	0.00151
mr30c15	LIZ3 23	0.50630	0.00238	13.59410	0.06117	0.19471	0.00051
Spot	Age 206/238	2σ	Age 207/235	2σ	Age 207/206	2σ	Conc %
mr30f10	531	5	547	11	614	13	86
mr30f08	545	6	556	10	602	10	91
mr30f13	545	16	560	27	616	35	88
mr30e16	546	12	542	22	524	18	104
mr30c11	548	10	556	16	586	16	94
mr30f11	548	9	551	23	560	24	98
mr30e05	553	5	557	15	570	14	97
mr30e09	563	9	551	14	500	12	113
mr30f09	567	9	573	9	592	11	96
mr30b10	569	8	568	12	564	14	101
mr30b12	572	6	588	17	646	20	89
mr30f12	576	7	596	17	670	23	86
mr30d08	577	15	580	19	592	22	97
mr30d11	590	9	591	14	592	15	100
mr30b14	593	10	583	14	542	14	109
mr30c12	594	6	606	9	650	10	91
mr30c05	596	13	602	17	628	20	95
mr30c10	597	15	616	16	684	12	87
mr30f06	597	11	601	12	612	16	98
mr30e11	598	8	605	21	632	18	95
mr30b09	600	12	605	12	622	9	96
mr30f15	602	10	611	17	644	16	93
mr30b13	604	8	607	20	616	21	98
mr30e15	607	10	615	14	646	18	94
mr30e12	608	16	618	33	650	43	94
mr30c07	609	12	610	14	614	11	99
mr30c08	610	14	605	18	586	15	104
mr30d14	612	13	601	18	556	17	110
mr30f05	615	20	615	23	612	26	100
mr30b11	616	7	626	13	658	15	94
mr30e13	617	9	610	13	584	10	106
mr30c14	618	6	627	15	660	16	94
mr30d06	627	9	626	18	618	16	101
mr30d10	631	10	628	15	616	15	102
mr30e06	632	11	633	19	634	18	100
mr30e14	633	10	619	19	566	16	112
mr30d16	646	14	642	21	626	13	103
mr30b08	1,338	16	1,415	18	1,532	15	87

Table 5 continued

Spot	Age 206/238	2σ	Age 207/235	2σ	Age 207/206	2σ	Conc %
mr30e10	1,485	16	1,496	17	1,510	20	98
mr30f07	1,639	29	1,685	51	1,740	57	94
mr30d09	1,773	22	1,779	28	1,786	27	99
mr30d15	1,879	24	1,912	34	1,948	27	96
mr30e07	1,928	12	1,980	16	2,032	14	95
mr30c09	1,982	31	2,028	37	2,074	17	96
mr30b07	2,028	22	2,071	22	2,112	23	96
mr30d05	2,038	30	2,074	23	2,108	17	97
mr30d13	2,064	25	2,137	41	2,206	37	94
mr30f16	2,221	31	2,292	71	2,354	80	94
mr30b05	2,319	23	2,399	37	2,466	46	94
mr30c15	2,641	25	2,722	24	2,782	14	95

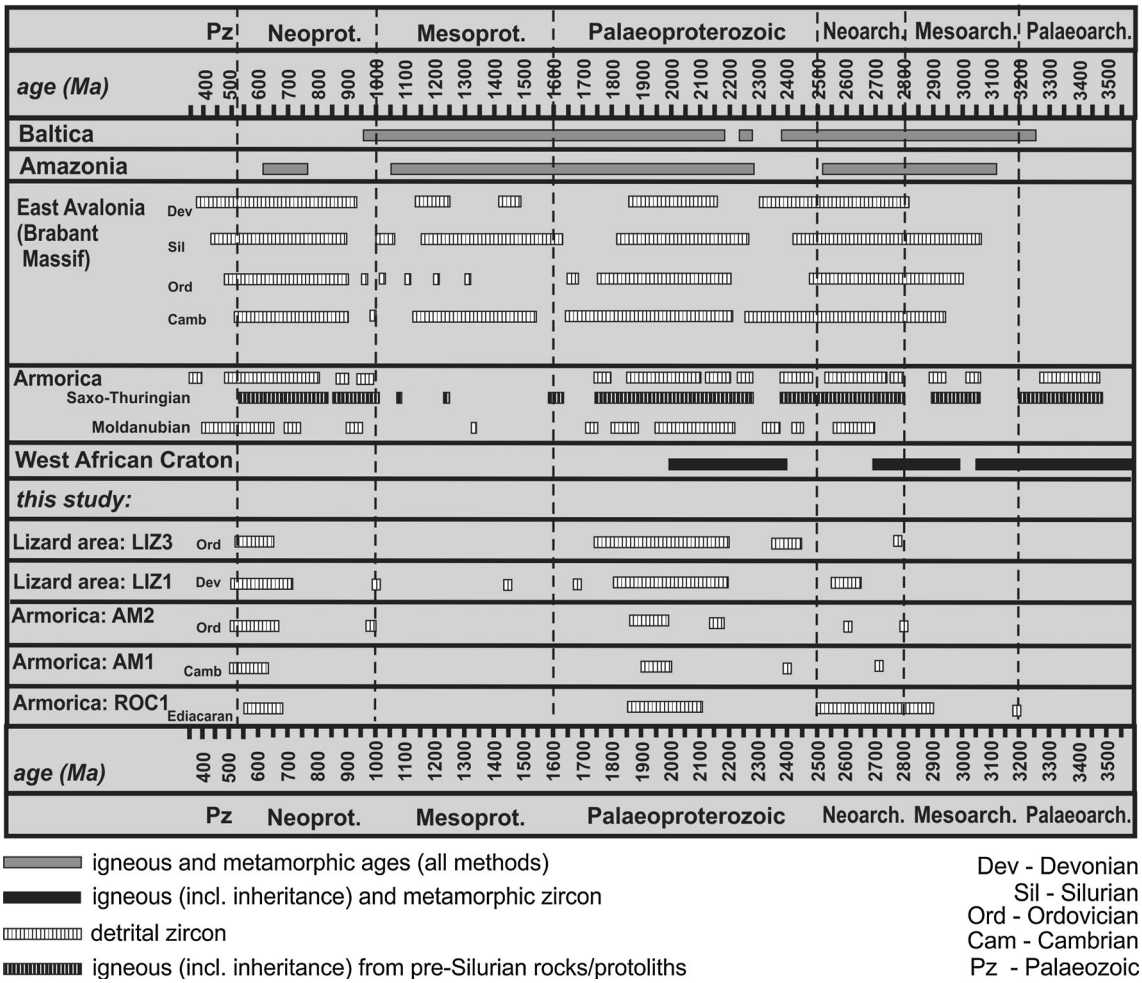

Fig. 11 Detrital zircon age distributions: the samples studied in this paper together with zircon age distributions of Baltica, Amazonia, East Avalonia (Brabant massif), Armorica (Cadomian basement in the Saxothuringian and Moldanubian zones, Bohemian Massif), and the West African craton (data compilation from Drost et al. 2011; Linnemann et al. 2004, 2008). Note the general occurrence of Mesoproterozoic zircon ages in Baltica, Amazonia and Avalonia and the contrasting rarity of the same zircon populations in Armorica (Cadomia) and the West African craton

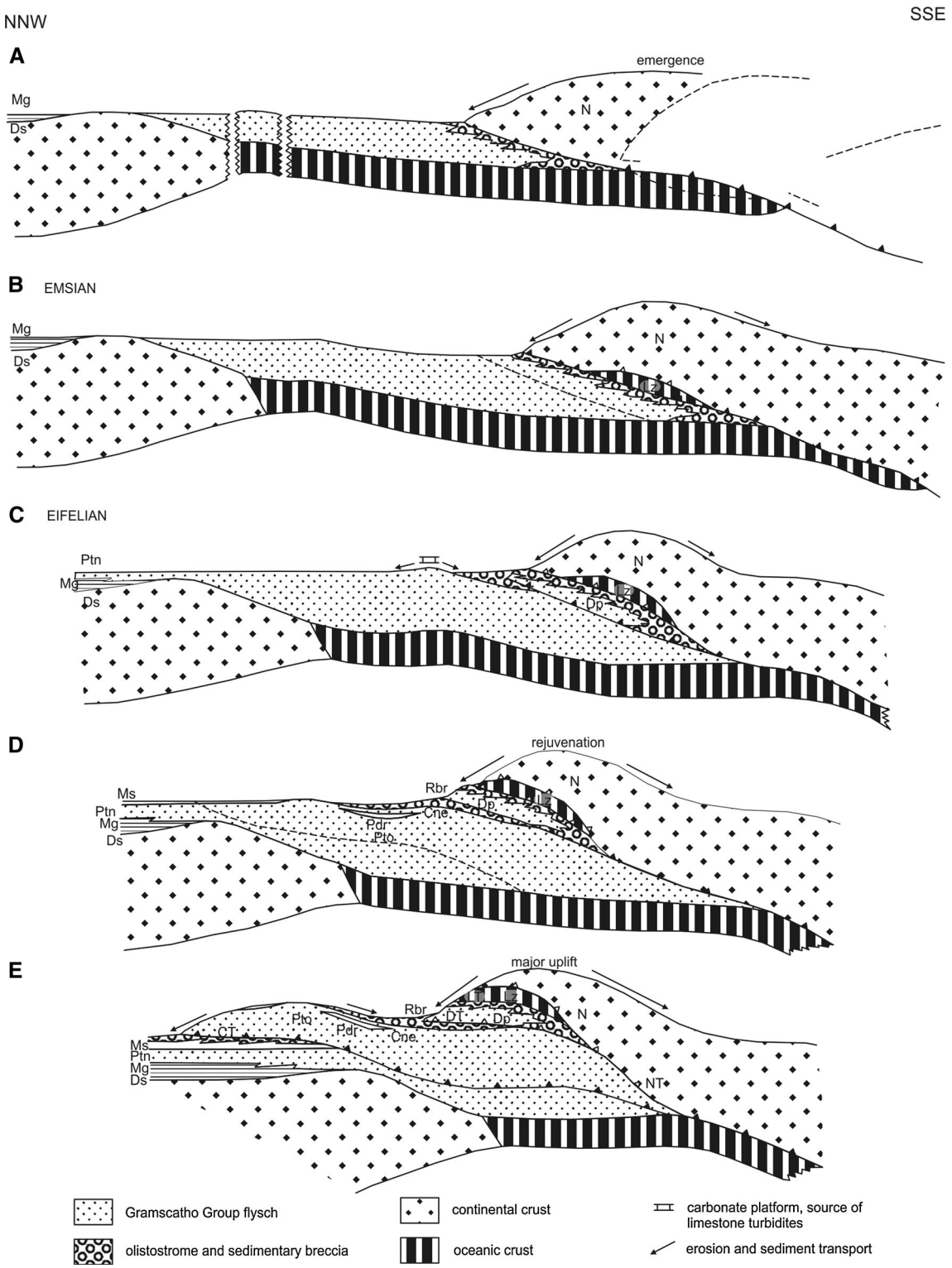

Fig. 12 A model for the Devonian tectonic evolution of the Lizard ophiolite complex in South Cornwall, depicting the progressive erosion of advancing thrust nappes of the Armorican plate (*right*) onto the southern margin of Avalonia (*left*) (from Holder and Leveridge 1986). *Cne* Carne Formation, *Ds* Dartmouth Slates, *Mg* Meadfoot Group, *Ms* Mylor Slate Formation, *Pd* Pendower Formation, *Pto* Portscatho Formation, *Ptn* Porthtowan Formation, *Rbr*-Roseland Breccia Formation. Tectonic units: Ck-Carrick Nappe, CT-Carrick Thrust, DP-Dodman Nappe, DT-Dodman Thrust, LT-Lizard Thrust, Lz-Lizard Nappe, N-Normannian Nappe, NT-Normannian Thrust

Formation by Dörr et al. (1999). However, our new data set does not contain any evidence for detrital zircons of this age. Detrital zircons analysed from the matrix of the Meneage Formation therefore only provide a partial picture of the composition of the over-riding Armorican plate in the vicinity of the Rheic suture.

Acknowledgments The authors acknowledge the discussion in the field with participants of the IGCP 497 fieldtrip to SW England in July 2005, and the reviews from James Braid and Nigel Woodcock that improved the paper.

References

Ballevre M, Bosse V, Ducassou C, Pitra P (2009) Palaeozoic history of the Armorican Massif: models for the tectonic evolution of the suture zones. CR de Geosci 341:174–201

Barnes RP (1983) The stratigraphy of a sedimentary melange and associated deposits in South Cornwall. Engl Proc Geol Assoc 94:217–229

Barnes RP, Andrews JR (1984) Hot or cold emplacement of the Lizard Complex? J Geol Soc Lond 141:37–39

Barnes RP, Andrews JR (1986) Upper Palaeozoic ophiolite generation and obduction in south Cornwall. J Geol Soc Lond 143:117–124

Bertrand L (1921) Les anciennes mers de la France et leur deposits. Flammarion, Paris

BIRPS & ECORS (1986) Deep seismic reflection profiling between England, France and Ireland. J Geol Soc Lond 143:45–52

Bluck BJ, Haughton PDW, House MR, Selwood EB, Tunbridge IP (1988) Devonian of England, Wales and Scotland. In: McMillan NJ, Embry AF, Glass DJ (eds) Devonian of the World. Mem Canad Soc Petrol Geol 14:305–324

Bluck BJ, Cope JCW, Scrutton CT (1992) Devonian. In: Cope JCW, Ingham JK, Rawson, PF (eds) Atlas of palaeogeography and lithofacies. Geol Soc, Lond 57–66

Bromley AV (1979) Ophiolitic origin of the Lizard Complex. J Camborne Sch Mines 79:25–38

Calvez JY, Vidal P (1978) Two billion years old relicts in the Hercynian belt of Western Europe. Contrib Mineral Petrol 65:395–399

Cawood PA, Nemchin AA, Smith M, Loewy S (2003) Source of the Dalradian Supergroup constrained by U–Pb dating of detrital zircon and implications for the East Laurentian margin. J Geol Soc Lond 160:231–246

Cawood PA, Nemchin AA, Strachan RA, Kinny PD, Loewy S (2004) Laurentian provenance and tectonic setting for the upper Moine Supergroup, Scotland, constrained by detrital zircons from the Loch Eil and Glen Urquhart successions. J Geol Soc Lond 161:863–874

Cawood PA, Nemchin AA, Strachan RA, Prave AR, Krabbendam M (2007) Sedimentary basin and detrital zircon record along East Laurentia and Baltica during assembly and breakup of Rodinia. J Geol Soc Lond 164:257–275

Chantraine J, Auvray B, Rabu D (1994) The Cadomian orogeny in the Armorican massif: igneous activity. In: Keppie JD (ed) Pre-mesozoic geology in France. Springer, Berlin, pp 111–125

Chen Y, Clark AH, Farrar E, Wasteneys HAHP, Hodgson MJ, Bromley AV (1993) Diachronous and independent histories of plutonism and mineralization in the Cornubian Batholith, southwest England. J Geol Soc Lond 150:1183–1191

Chesley JT, Halliday AN, Snee LWE, Mezger K, Shepherd TJ, Scrivener RC (1993) Thermochronology of the Cornubian batholith in southwest England: implications for pluton emplacement and protracted hydrothermal mineralization. Geochim Cosmochem Acta 57:1817–1835

Clark AH, Scott DJ, Sandemann HA, Bromley AV (1998) Siegenian generation of the Lizard ophiolite: U–Pb zircon age data for plagiogranite, Porthkerris, Cornwall. J Geol Soc Lond 155:595–598

Cocks LRM, Torsvik TH (2002) Earth geography from 500 to 400 million years ago: a faunal and palaeomagnetic review. J Geol Soc Lond 159:631–644

Cogné J (1990) The Cadomian orogeny and its influence on the Variscan evolution of western Europe. In: D'Lemos RS, Strachan RA, Topley CG (eds) The Cadomian Orogeny. Geol Soc Lond, Spec Pub 51:305–311

Collins AS, Buchan C (2004) Provenance and ago constraints of the South Stack Group, Anglesey, UK: U–Pb SIMS detrital zircon data. J Geol Soc Lond 161:743–746

Coward MP, McClay KR (1983) Thrust tectonics of S Devon. J Geol Soc Lond 140:215–228

Dodson MH, Compston W, Williams IS, Wilson JF (1988) A search for ancient detrital zircons in Zimbabwean sediments. J Geol Soc Lond 145:977–983

Doré F (1994) Cambrian of the Armorican massif. In: Keppie JD (ed) Pre-mesozoic geology in France. Springer, Berlin, pp 136–141

Dörr W, Floyd PA, Leveridge BE (1999) U–Pb ages and geochemistry of granite pebbles from the Devonian Menaver Conglomerate, Lizard peninsula: provenance of Rhenohercynian flysch of SW England. Sed Geol 124:131–147

Drost K, Gerdes A, Jeffries T, Linnemann U, Storey C (2011) Provenance of Neoproterozoic and early Palaeozoic siliciclastic rocks of the Teplá-Barrandian unit (Bohemian Massif): evidence from U–Pb detrital zircon ages. Gondwana Res 19:213–231

Egal E, Guerrot C, Le Goff E, Thieblemont D, and Chantraine J (1996) The Cadomian orogen revisited in North Brittany. In: Nance RD, Thompson MD (eds) Avalonian and Related Peri-Gondwanan Terranes of the Circum-Atlantic. Geol Soc Am, Spec Pap 304:281–318

Fernández-Suárez J, Gutiérrez-Alonso G, Cox R, Jenner GA (2002a) Assembly of the Armorica microplate: a strike-slip terrane delivery? Evidence from U–Pb ages of detrital zircons. J Geol 110:619–626

Fernández-Suárez J, Gutiérrez-Alonso G, Jeffries TE (2002b) The importance of along-margin terrane transport in northern Gondwana: insights from detrital zircon parentage in Neoproterozoic rocks from Iberia and Brittany. Earth Planet Sci Lett 204:75–88

Floyd PA (1984) Geochemical characteristics and comparison of the basic rocks of the Lizard Complex and the basaltic lavas within the Hercynian troughs of SW England. J Geol Soc Lond 144:531–542

Floyd PA, Leveridge BE (1987) Tectonic environment of the Devonian Gramscatho basin, south Cornwall: framework mode and geochemical evidence from turbiditic sandstones. J Geol Soc Lond 144:531–542

Friedl G, Finger F, McNaughton NJ, Fletcher IR (2000) Deducing the ancestry of terranes: SHRIMP evidence for South America-derived Gondwana fragments in central Europe. Geology 28:1035–1038

Gibbons W, Thompson L (1991) Ophiolitic mylonites in the Lizard Complex: ductile extension in the lower crust. Geology 19:1009–1012

Hartley AJ (1993) Silesian sedimentation in southwest Britain: sedimentary responses to the developing Variscan orogeny. In: Gayer R, Greiling RO, Vogel AK (eds) Rhenohercynian and subvariscan fold belts. Vieweg, Wiesbaden/Braunschweig, pp 160–196

Holder MT, Leveridge BE (1986) A model for the tectonic evolution of south Cornwall. J Geol Soc Lond 143:125–134

Jeffries TE, Fernandez-Suárez J, Corfu F, Gutiérrez-Alonso G (2003) Advances in U–Pb geochronology using frequency quintupled Nd:YAG based laser ablation system and quadrupole based ICP-MS. J Anal At Spect 18:847–855

Keppie JD, Nance RD, Murphy JB, Dostal J (2003) Tethyan, Mediterranean and Pacific analogues for the Neoproterozoic-Palaeozoic birth and development of peri-Gondwanan terranes and their transfer to Laurentia and Laurussia. Tectonophysics 365:195–219

Le Gall B (1990) Evidence of an imbricate thrust belt in the southern British Variscides: contributions of South-Western approaches traverse (SWAT) deep seismic reflection profiling recorded through the English Channel. Tectonics 9:283–302

Leveridge BE, Holder MT, Day GA (1984) Thrust nappe tectonics in the Devonian of south Cornwall and the western English Channel. In: Hutton DHW, Sanderson DJ (eds) Variscan Tectonics of the North Atlantic Region. Geol Soc Lond, Spec Pub 14:103–112

Linnemann U, McNaughton NJ, Romer RL, Gehmlich M, Drost K, Tonk C (2004) West African provenance for Saxo-Thuringia (Bohemian Massif): did Armorica ever leave pre-Pangean Gondwana?-U–Pn SHRIMP zircon evidence and the Nd-isotopic record. Int J Earth Sci 93:683–705

Linnemann U, D'Lemos RS, Drost K, Jeffries T, Gerdes A, Romer RL, Samson SD, Strachan RA (2008) Cadomian tectonics. In: McCann T (ed) The geology of Central Europe, volume 1: precambrian and Palaeozoic. Geol Soc Lond 103–154

Ludwig KR (2001) SQUID 1.00: A user's manual. Berkeley Geochronology Centre Special Publication 2, p 19

Matte P (1986) Tectonics and plate tectonic models for the Variscan belt of Europe. Tectonophysics 126:329–374

Murphy JB, Nance RD (1989) Model for the evolution of the Avalonian-Cadomian belt. Geology 17:735–738

Murphy JB, Nance RD (1991) Supercontinent model for the contrasting character of Late Proterozoic orogenic belts. Geology 19:469–472

Murphy JB, Strachan RA, Nance RD, Parker KD, Fowler MB (2000) Proto-Avalonia: a 1.2–1.0 Ga tectonothermal event and constraints for the evolution of Rodinia. Geology 29:1071–1074

Murphy JB, Fernández-Suárez J, Jeffries TE, Strachan RA (2004) U–Pb (LA–ICP-MS) dating of detrital zircons from Cambrian clastic rocks in Avalonia: erosion of a Neoproterozoic arc along the northern Gondwanan margin. J Geol Soc Lond 161:243–254

Nance RD, Murphy JB, Strachan RA, D'Lemos RS, Taylor GK (1991) Late Proterozoic tectonostratigraphic evolution of the Avalonian and Cadomian terranes. Precam Res 53:41–78

Nance RD, Murphy JB, Keppie JD (2002) Cordilleran model for the evolution of Avalonia. Tectonophysics 352:11–31

Nance RD, Murphy JB, Strachan RA, Keppie JD, Gutiérrez-Alonso G, Fernández-Suárez J, Quesada C, Linnemann U, D'Lemos RS, Pisarevsky SA (2007) Neoproterozoic-early Palaeozoic tectonostratigraphy and palaeogeography of the peri-Gondwanan terranes: Amazonian versus West African connections. In: Nasser E,Liégeois J-P (eds) The Boundaries of the West African Craton. Geol Soc Lond, Spec Pub 297:345–383

Nance RD, Gutiérrez-Alonso G, Keppie JD, Linnemann U, Murphy JB, Quesada C, Strachan RA, Woodcock NH (2010) Evolution of the Rheic Ocean. Gondwana Res 17:194–222

Pickering KT, Bassett MG, Siveter DJ (1988) Late Ordovician-Early Silurian destruction of the Iapetus Ocean: newfoundland, British Isles and Scandinavia—a discussion. Trans Roy Soc Edin Earth Sci 79:361–382

Rabu D, Chantraine J, Chauvel JJ, Denis E, Balé P, Bardy Ph (1990) The Brioverian (Upper Proterozoic) and the Cadomian orogeny in the Armorican Massif. In: D'Lemos RS, Strachan RA, Topley CG (eds) The Cadomian Orogeny. Geol Soc Lond, Spec Pub 51:81–94

Rainbird RH, Hamilton MA, Young GM (2001) Detrital zircon geochronology and provenance of the Torridonian, NW Scotland. J Geol Soc Lond 158:15–27

Robardet M, Bonjour JL, Paris F, Morzadec P, Racheboeuf PR (1994) In: Keppie JD (ed) Pre-mesozoic geology in France. Springer, Berlin, pp 142–151

Roberts S, Andrews JR, Bull JM, Sanderson DJ (1993) Slow-spreading ridge-axis tectonics: evidence from the Lizard Complex, UK. Earth Planet Sci Lett 116:101–112

Sadler PM (1974) Trilobites from the Gorran quartzites, Ordovician of south Cornwall. Palaeontology 17:71–93

Samson SD, D'Lemos RS (1998) U–Pb geochronology and Sm–Nd isotopic composition of Proterozoic gneisses, Channel Islands, UK. J Geol Soc Lond 155:609–618

Samson SD, D'Lemos RS, Miller BV, Hamilton MA (2005) Neoproterozoic palaeogeography of the Cadomia and Avalon terranes: constraints from detrital zircon U–Pb ages. J Geol Soc Lond 162:65–71

Sanderson DJ (1984) Structural variations across the northern margin of the Variscides in NW Europe. In: Hutton DHW, Sanderson DJ (eds) Variscan Tectonics of the North Atlantic Region. Geol Soc Lond, Spec Pub 14:149–165

Seago RD, Chapman TJ (1988) The confrontation of structural styles and the evolution of a foreland basin in central SW England. J Geol Soc Lond 145:789–800

Shackleton RM, Ries AC, Coward MP (1982) An interpretation of the Variscan structures in SW England. J Geol Soc Lond 139:533–541

Sircombe KN (2000) Quantitative comparison of geochronological data using multivariate analysis: a provenance study example from Australia. Geochim Cosmochim Acta 64:1593–1619

Sircombe KN (2004) AgeDisplay: an EXCEL workbook to evaluate and display univariate geochronological data using binned frequency histograms and probability density distributions. Comput Geosci 30:21–31

Soper NJ, Strachan RA, Holdsworth RE, Gayer RA, Greiling RO (1992) Sinistral transpression and the Silurian closure of Iapetus. J Geol Soc Lond 14:871–880

Stampfli GM, Borel GD (2002) A plate tectonic model for the Palaeozoic and Mesozoic constrained by dynamic plate boundaries and restored synthetic oceanic isochrones. Earth Planet Sci Lett 196:17–33

Strachan RA, D'Lemos RS, Dallmeyer RD (1996) Neoproterozoic evolution of an active plate margin: North Armorican Massif, France. In: Nance RD, Thompson MD (eds) Avalonian and Related Peri-Gondwanan Terranes of the Circum-Atlantic. Geol Soc Am, Spec Pap 304:319–332

Strachan RA, Collins AS, Buchan C, Nance RD, Murphy JB, D'Lemos RS (2007) Terrane analysis along a Neoproterozoic active margin of Gondwana: insights from U–Pb zircon geochronology. J Geol Soc Lond 164:57–60

Styles MT, Kirby GA (1980) New investigation of the Lizard Complex, Cornwall, and discussion of an ophiolite model. In: Panayiotou A (ed) Ophiolites: proceedings of the international ophiolite symposium, Cyprus, 1979. Geological Survey Department, Nicosia, pp 517–526

Taylor GK, Strachan RA (1990) Palaeomagnetism and tectonic models for Avalonian-Cadomian geology of the North Atlantic. In: Strachan RA, Taylor GK (eds) Avalonian-Cadomian geology of the North Atlantic. Blackie, Glasgow, pp 237–247

Van Staal CR, Dewey JF, MacNiocaill C, McKerrow WS (1998) The Cambrian-Silurian tectonic evolution of the Northern Appalachians and British Caledonides: History of a complex west and

southwest Pacific-type segment of Iapetus. In: Blundell D, Scott AC (eds) Lyell: The present is the key to the past. Geol Soc Lond, Spec Pub 143:199–242

Vearncombe JR (1980) The Lizard ophiolite and two phases of sub-oceanic deformation. In: Panayiotou A (ed) Ophiolites: proceedings of the international ophiolite symposium, Cyprus, 1979. Geological Survey Department, Nicosia, pp 527–537

Wiedenbeck M, Allé P, Corfu F, Griffin WL, Meier M, Oberli F, von Quadt A, Roddick JC, Spiegel W (1995) Three natural zircon standard for U-Th-Pb, Lu-Hf, trace element and REE analyses. Geostand Newsl 19:1–23